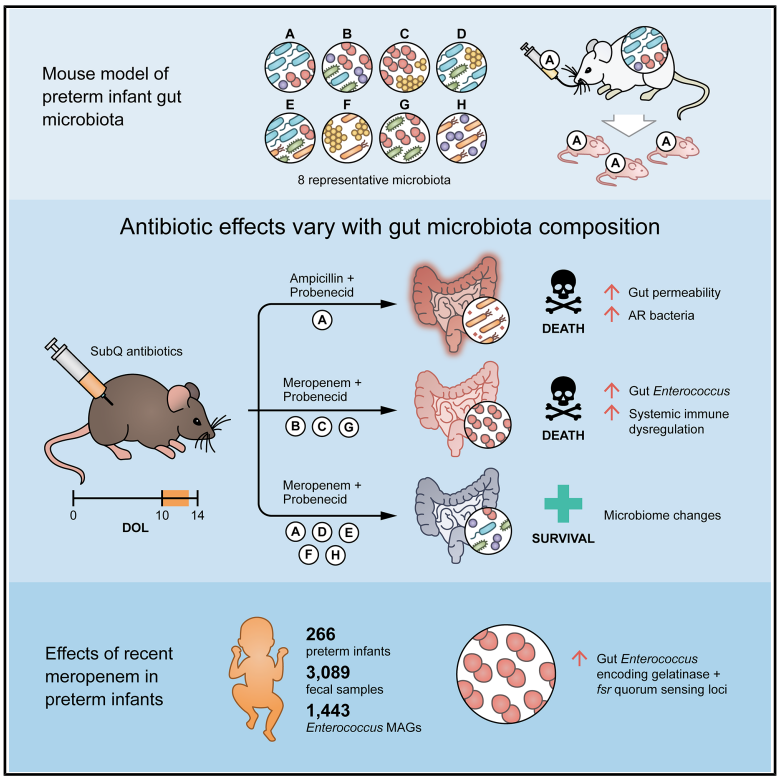
Cell Reports
Medicine

Article

Microbiome-antibiotic-immune interactions influence mortality in preterm infant gut microbiota-humanized gnotobiotic mice

Graphical abstract



Highlights

- Preterm infant gut microbiomes are dominated by potential pathogens
- Microbiome-humanized mouse pups die during specific antibiotic + probenecid treatment
- Death during meropenem + probenecid is associated with *gelE/fsr Enterococcus faecalis*
- *Enterococcus faecalis* increases in abundance in human infant guts after meropenem

Authors

Drew J. Schwartz, Galen G. Wong, Kate E. Wardenburg, ..., Barbara B. Warner, Phillip I. Tarr, Gautam Dantas

Correspondence

schwartzd@wustl.edu (D.J.S.), dantas@wustl.edu (G.D.)

In brief

Preterm infants are commonly treated with antibiotics. Schwartz et al. discover associations between antibiotic administration, systemic immune responses, microbiome composition, and death in gnotobiotic mouse pups humanized with stool from preterm infants. These findings can help contextualize the unintended consequences of antibiotic administration for preterm infants.

Schwartz et al., 2026, Cell Reports Medicine 7, 103161
November 17, 2026 © 2026 The Author(s). Published by Elsevier Inc.
https://doi.org/10.1016/j.xcrm.2026.103161

CellPress

Please cite this article in press as: Schwartz et al., Microbiome-antibiotic-immune interactions influence mortality in preterm infant gut microbiota-humanized gnotobiotic mice, Cell Reports Medicine (2026), https://doi.org/10.1016/j.xcrm.2026.103161

Cell Reports Medicine

CellPress
OPEN ACCESS

Article

Microbiome-antibiotic-immune interactions influence mortality in preterm infant gut microbiota-humanized gnotobiotic mice

Drew J. Schwartz,[1,2,3,4,5,*] Galen G. Wong,[1,4,5] Kate E. Wardenburg,[5] Isabel R. Erickson,[1,2,4] Jessica Tung,[1,2,4] Jie Ning,[5,6] Lingxia Zhao,[1,4] Nitan Shalon,[5] Alaric W. D'Souza,[5] Aura Ferreiro,[1,4] Rachel B. Silverstein,[1,2,4] Terence S. Crofts,[5,7] Carla Hall-Moore,[1] Meghan A. Wallace,[6] John I. Robinson,[4,8] Jeffrey P. Henderson,[2,4,8] Carey-Ann D. Burnham,[1,2,6] Barbara B. Warner,[1] Phillip I. Tarr,[1,2] and Gautam Dantas[1,2,5,6,9,10,*]

[1]Department of Pediatrics, Washington University School of Medicine, St. Louis, MO 63110, USA
[2]Department of Molecular Microbiology, Washington University School of Medicine, St. Louis, MO 63110, USA
[3]Department of Obstetrics & Gynecology, Washington University School of Medicine, St. Louis, MO 63110, USA
[4]Center for Women's Infectious Disease Research, Washington University School of Medicine, St. Louis, MO 63110, USA
[5]The Edison Family Center for Genome Sciences and Systems Biology, Washington University School of Medicine, St. Louis, MO 63110, USA
[6]Department of Pathology & Immunology, Division of Laboratory and Genomic Medicine, Washington University School of Medicine, St. Louis, MO 63110, USA
[7]Department of Animal Sciences, Carl R. Woese Institute for Genomic Biology, Division of Nutritional Sciences, University of Illinois, Urbana-Champaign, IL, USA
[8]Department of Medicine, Washington University School of Medicine, St. Louis, MO 63110, USA
[9]Department of Biomedical Engineering, Washington University in St. Louis, St. Louis, MO, USA
[10]Lead contact
*Correspondence: schwartzd@wustl.edu (D.J.S.), dantas@wustl.edu (G.D.)
https://doi.org/10.1016/j.xcrm.2026.103161

SUMMARY

Infants born preterm are treated with antibiotics when bacterial infection is suspected. Antibiotics disrupt the gut microbiota, leading to unfavorable immune and infectious consequences. However, the impact of specific antibiotics on gut microbial and immune responses is largely unknown. We develop a humanized gnotobiotic mouse model where we gavage preterm infant stool into germ-free dams. We treat microbiota-humanized pups with subcutaneous antibiotics with probenecid to model empiric sepsis treatment regimens. Pups humanized with microbiota including ampicillin-resistant *Enterobacteriaceae* die during ampicillin with probenecid treatment with increased gut permeability and systemic microbial spread. Conversely, pups with microbiota containing gelatinase-expressing *Enterococcus faecalis* die during meropenem with probenecid treatment with increased gut *E. faecalis* and systemic immune dysregulation. Gut *E. faecalis*, especially strains containing *gelE* and *fsr*, increase in human preterm infant gut microbiomes after meropenem. These data raise concerns about the unintended consequences of antibiotic treatment and provide a framework for understanding microbiome-antibiotic-immune interplay.

INTRODUCTION

Preterm infants hospitalized in neonatal intensive care units (NICUs) are susceptible to sepsis with an associated 17% mortality.[1] Late-onset sepsis (LOS), a dysregulated immune response from suspected or confirmed infection after 3 days of life (DOL), affects up to 20% of extremely-low-birthweight infants.[1–4] Bacterial bloodstream infections frequently cause LOS in NICUs and are usually attributed to *Enterobacteriaceae*, *Staphylococcaceae*, and *Enterococcaceae*.[4] These families are highly prevalent in, and often dominate, the preterm infant gut microbiota with >50% relative abundance.[5,6] Furthermore, identical strains of bacteria colonize the preterm infant gut microbiota and increase in abundance prior to bloodstream infection and LOS, suggesting that the gut microbiome is a habitat for sepsis pathogens.[7–9] Preterm infant gut bacterial communities are highly dynamic in the first month of life and undergo microbiota shifts that introduce potentially pathogenic species while depleting beneficial colonizers.[6,7] Thus, the neonatal gut microbiota is a dynamically changing environment that can be a source of bacteria causing LOS.

Because of the risk of bacterial LOS, >80% of hospitalized preterm infants are treated with antibiotics.[10] Yet, these antibiotics disrupt the developing gut microbiota, often dramatically altering the abundance of potential LOS pathogens.[6–8,11] Prior antibiotic exposure is a risk factor for developing LOS, including episodes caused by antibiotic-resistant bacteria.[12–14] Sepsis with sterile cultures (i.e., culture-negative sepsis) and prolonged

This is an open access article under the CC BY-NC-ND license (http://creativecommons.org/licenses/by-nc-nd/4.0/).

Please cite this article in press as: Schwartz et al., Microbiome-antibiotic-immune interactions influence mortality in preterm infant gut microbiota-humanized gnotobiotic mice, Cell Reports Medicine (2026), https://doi.org/10.1016/j.xcrm.2026.103161

antibiotic exposure are also associated with multiple adverse inflammatory outcomes including necrotizing enterocolitis and death.[14–18] Interventions accompanying preterm birth that alter the gut microbiota including antibiotic exposure, non-antibiotic medications, prolonged hospital admission, and changes in standard feeding patterns are associated with acute and chronic systemic inflammatory changes.[19–21] The impact of specific antibiotics on the host and microbiota is challenging to predict, likely due to the combinatorial influences of these variables and the dynamic nature of the neonatal gut microbiota and immune system.[6,11,19,22] Understanding the impacts of specific and common antibiotics on the preterm infant host can help predict and prevent poor outcomes.

Distinguishing preterm neonates with culture-positive sepsis, culture-negative sepsis, and without sepsis is challenging. While the concentrations of several circulating biomarkers such as interleukin (IL)-6, C-reactive protein (CRP), and tumor necrosis factor (TNF)-α can partly distinguish these conditions, inflammatory markers are non-specific with variable sensitivity.[23,24] Further, antibiotic exposure is associated with gut microbiota and inflammatory changes in stool.[25] Thus, even without overt sepsis, antibiotic treatment can affect the gut microbiota and intestinal biology leading to local and systemic immune changes.

Animal models can illuminate the consequences of disrupting the gut microbiota-immune-antibiotic axis. Pups of conventional dams treated with gentamicin were more susceptible to *Klebsiella* sepsis compared to vancomycin-treated dams.[26] Similarly, perinatal antibiotic exposure in dams disrupted the neonatal gut microbiota and immune development in an antibiotic-specific fashion.[27,28] Ampicillin, vancomycin, and neomycin facilitated commensal and pathogenic bacterial translocation into mesenteric lymph nodes by opening colonic goblet cell-associated antigen passages.[29,30] While informative, these and other models differ substantially from human preterm infant antibiotic and microbial exposures. First, antibiotics are often administered to dams with pups acquiring antibiotics in breastmilk, unlike in human infants, who receive them intravenously. Parenteral administration dramatically alters serum concentrations and differentially impacts the gut microbiota and antibiotic resistance gene repertoire.[31] Second, the microbiota of conventional mice differs significantly from human infants.[6,26,32] Third, infectious agents are administered exogenously via injection in many animal models, unlike in preterm infants where the causative strain often emerges from the gut.[7,8] Finally, cecal slurry injection models recapitulate spontaneous intestinal perforation or necrotizing enterocolitis with polymicrobial bacteremia[33,34] and not the common phenomenon of culture-negative or monomicrobial culture-positive LOS.[15,16]

To model relevant preterm infant microbial and antibiotic exposures, we present a gnotobiotic mouse model of infant gut microbiota development and antibiotic-mediated disruption. We considered many features essential for modeling antibiotic impacts on the human neonatal gut microbiota. First, we used stool from human preterm infants as the inoculum. We verified that bacteria in these samples are vertically transmitted to pups after colonization of germ-free dams. Second, because antibiotic delivery to hospitalized preterm infants is primarily intravenous,[35] we aimed to achieve serum concentrations approximating those in serum of human infants after systemic administration. Finally, because antibiotics variably impact the gut microbiota, gut permeability, and clinical outcomes,[6,11,15,36] we wanted to reproduce this variability in our model.

Overall, we hypothesized that antibiotic effects would depend on the pup gut microbiota composition. Using eight fecal samples representative of human preterm infant gut microbiota, we identified associations between microbial composition and antibiotic exposure with culture-positive sepsis, culture-negative sepsis, and microbiota disruption without mortality. Finally, we demonstrate that key microbiota changes we observe in humanized gnotobiotic mouse pups occur in a cohort of 3,089 previously sequenced fecal samples from 266 hospitalized preterm infants from the central United States.

RESULTS

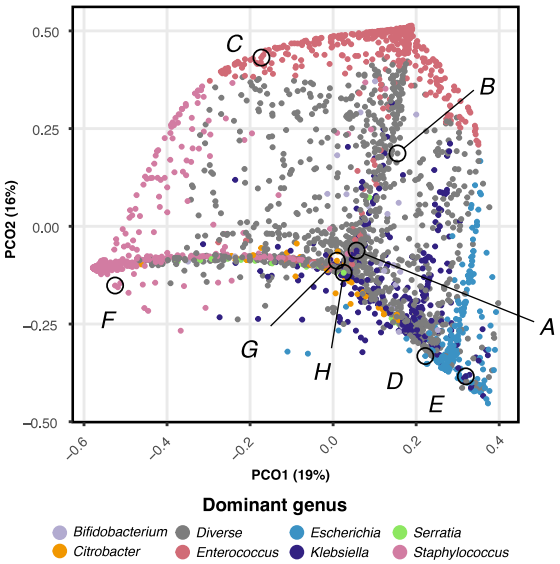
Identification of representative fecal samples from a human cohort

The human preterm gut microbiota is often dominated at >50% relative abundances of genera from the *Enterobacteriaceae*, *Enterococcaceae*, and *Staphylococcaceae* families, which commonly cause bloodstream infection and sepsis.[2,5–8] Unlike their breastfed term counterparts, *Bifidobacterium* dominance is uncommon in hospitalized preterm infants.[5,6] To identify representative bacterial compositions, we analyzed previously metagenomically sequenced samples from a cohort of 977 hospitalized preterm neonates in three NICUs in the midwestern United States (Data S1 and S2).[6,7,11,37–39] Because the infant gut microbiota is most dynamic in early life,[5,6] we focused on 2,912 samples from 262 subjects in the first 60 DOL.[6,7,11,39] We used principal coordinate analysis (PCoA) of Bray-Curtis dissimilarity to separate fecal samples based on >50% dominant genus abundance (Figure 1A). *Staphylococcus*, *Enterococcus*, *Klebsiella*, *Escherichia*, *Citrobacter*, or *Serratia* was the dominant genus in 17% (n = 505), 17% (n = 488), 14% (n = 414), 9% (n = 272), 2% (n = 50), and 1% (n = 26) of the stools, respectively. *Bifidobacterium* dominance was only observed in 1% (30/2,912) of samples, consistent with other preterm infant studies.[5] The remaining stools (1,127/2,912) were classified as diverse, though they could have other genera at >50% abundance. We selected eight representative fecal samples, termed Microbiota A–H, that were variably dominated by these key genera (Figures 1A and 1B). Infants from whom these stools originated were representative of our cohort, born after an average of 27 weeks' completed gestation with near-universal antibiotic exposure in the first week of life (Figure 1B).[6,7,11,37–39] Microbiota A and E were dominated by *Klebsiella*, but they also contained putatively beneficial *Veillonella* (A) and *Bifidobacterium* (E) (Figure 1; Data S1 and S2). Microbiota B was diverse, consisting of *Enterococcus* (26%) and anaerobes including *Anaerococcus* (22%), *Varibaculum* (12%), and *Bifidobacterium* (7%) (Figure 1B; Data S1 and S2). Microbiota C was composed primarily of Gram-positive *Enterococcus* and *Staphylococcus*, whereas Microbiota D, G, and H consisted mostly of Enterobacterales (*Escherichia*, *Citrobacter*, and *Serratia*, respectively) (Figure 1B). Having identified our key fecal samples, we next sought to evaluate microbial colonization in germ-free mice.

Please cite this article in press as: Schwartz et al., Microbiome-antibiotic-immune interactions influence mortality in preterm infant gut microbiota-humanized gnotobiotic mice, Cell Reports Medicine (2026), https://doi.org/10.1016/j.xcrm.2026.103161

CellPress
OPEN ACCESS

A



B

	Microbiota A	Microbiota B	Microbiota C	Microbiota D
Gestational age	29 0/7	24 0/7	26 5/7	27 0/7
Sample DOL	27	21	12	15
Composition	82% *Klebsiella* 8% *Veillonella* 5% *Enterococcus*	26% *Enterococcus* 22% *Anaerococcus* 12% *Varibaculum*	65% *Enterococcus* 32% *Staphylococcus* 1% *Escherichia*	55% *Escherichia* 27% *Citrobacter* 14% *Staphylococcus*
Antibiotic history	DOL 0-2 Ampicillin Gentamicin	DOL 0-7 Ampicillin Gentamicin	DOL 0-1 Ampicillin Gentamicin DOL 11-12 Vancomycin Gentamicin	DOL 0 Gentamicin DOL 0-9 Penicillin

	Microbiota E	Microbiota F	Microbiota G	Microbiota H
Gestational age	25 0/7	26 3/7	26 4/7	25 0/7
Sample DOL	52	6	15	18
Composition	58% *Klebsiella* 25% *Escherichia* 7% *Bifidobacterium*	93% *Staphylococcus* 7% *Escherichia*	85% *Citrobacter* 10% *Leclercia* 1% *Enterococcus*	68% *Serratia* 31% *Bifidobacterium*
Antibiotic history	DOL 0 Gentamicin DOL 0-3 Ampicillin DOL 1-6 Cefotaxime DOL 3-6 Vancomycin	DOL 1-3 Ampicillin Gentamicin	DOL 0-7 Ampicillin Gentamicin	DOL 1-7 Ampicillin Gentamicin DOL 7-10 Vancomycin

Figure 1. The early-life gut microbiota is dominated by key genera

(A) PCoA of Bray-Curtis dissimilarity from $n = 2,912$ samples from $N = 262$ subjects in the first 60 DOL. Samples with ≥50% relative abundance of the listed genera are colorcoded.

(B) Eight representative samples used for gnotobiotic experiments and their relevant metadata. Sample identity is labeled in (A).

Establishment of microbiota humanization in gnotobiotic mouse pups

We colonized germ-free dams with the eight representative microbiota and evaluated colonization in pup fecal samples on DOL 10 with shotgun metagenomic sequencing. Individual inocula ranged from 2 to 20 species with Shannon diversity 0.2–2.4 (Figures S1A and S1B; Data S3 and S4). The mean number of species acquired ranged from 3 for Microbiota F- and G-humanized pups to 8 for Microbiota E-humanized pups (Figure S1A). Plating of inocula to MacConkey and Enterococcosel agar confirmed the presence of live microbes at the time of gavage into germ-free dams (Figure S1C). *Enterobacteriaceae*, *Enterococcaceae*, and *Staphylococcaceae*, consistently colonized the gut microbiome of pups at DOL 10. *Enterobacteriaceae* colonized at an average relative abundance of 99%, 81%, 77%, 57%, 33%, and 21% in Microbiota D, E, A, B, G, and H, respectively, and *Enterococcaceae* at 67%, 37%, 21%, 10%, and 4% in Microbiota G, C, B, E, and A, respectively (Figure 2A). *Staphylococcaceae* colonized Microbiota F-, C-, and D-humanized pups at 56%, 51%, and 1%, respectively. Key putatively beneficial microbes including *Bifidobacteriaceae*, *Veillonellaceae*, and obligate anaerobes such as *Clostridiaceae* and *Peptostreptococcaceae* also colonized infant pups at variable abundance (Figure 2A). We observed no statistically significant overall compositional differences with Bray-Curtis dissimilarity among samples from different microbiota or within microbiota between human inocula and DOL 10 mouse pup samples (PERMANOVA $p > 0.05$, Figure S1D; Data S4). Inocula and DOL 10 samples differed in V1 only for Microbiota C and in V2 for Microbiota A, suggesting high-fidelity engraftment of preterm infant fecal microbes in mouse pups (Benjamini-Hochberg [BH]-corrected Wilcox $q = 0.02$ and $q = 0.04$, respectively). Microbiota D-humanized pups harbored a median of 1.8×10^4 (interquartile range [IQR]: 3.3×10^4) colony-forming units (CFUs)/mg stool on MacConkey agar, significantly greater than CFUs on MacConkey agar for Microbiota B-, F-, and G-humanized pups (Figure 2B; Data S4). Meanwhile, the stool of Microbiota C- and G-humanized pups at DOL 10 contained 10^3–10^4 CFUs/mg *Enterococcus* vs. 10^1–10^2 CFUs/mg in Microbiota A-, B-, and E-humanized pups and limit of detection (LOD) in Microbiota D-, F-, and H-humanized pups. Overall, key taxa from the inoculum colonized pups with relative abundances like the human infant inocula. Importantly, fecal microbiota containing between 2 and 12 species is consistent with data from stools from hospitalized preterm infants.[6,7]

Serum antibiotic concentrations in conventional mouse pups approximate concentrations in human preterm infants

Empiric use for suspected sepsis is the most common indication for antibiotics for hospitalized infants worldwide.[40] β-Lactams, aminoglycosides, and vancomycin are the most frequently prescribed[35,40] and differentially affect the infant gut microbiota.[7,11] Critically ill neonates are often treated with meropenem,[40] a broad-spectrum carbapenem targeting Gram-negative and Gram-positive bacteria, including anaerobic bacteria.[41] To employ dosing regimens of commonly administered antibiotics in our model, we performed pharmacokinetic measurements in conventional mice. We subcutaneously injected pups at DOL 10 with increasing doses of ampicillin or meropenem and

CellPress
OPEN ACCESS

Cell Reports Medicine
Article

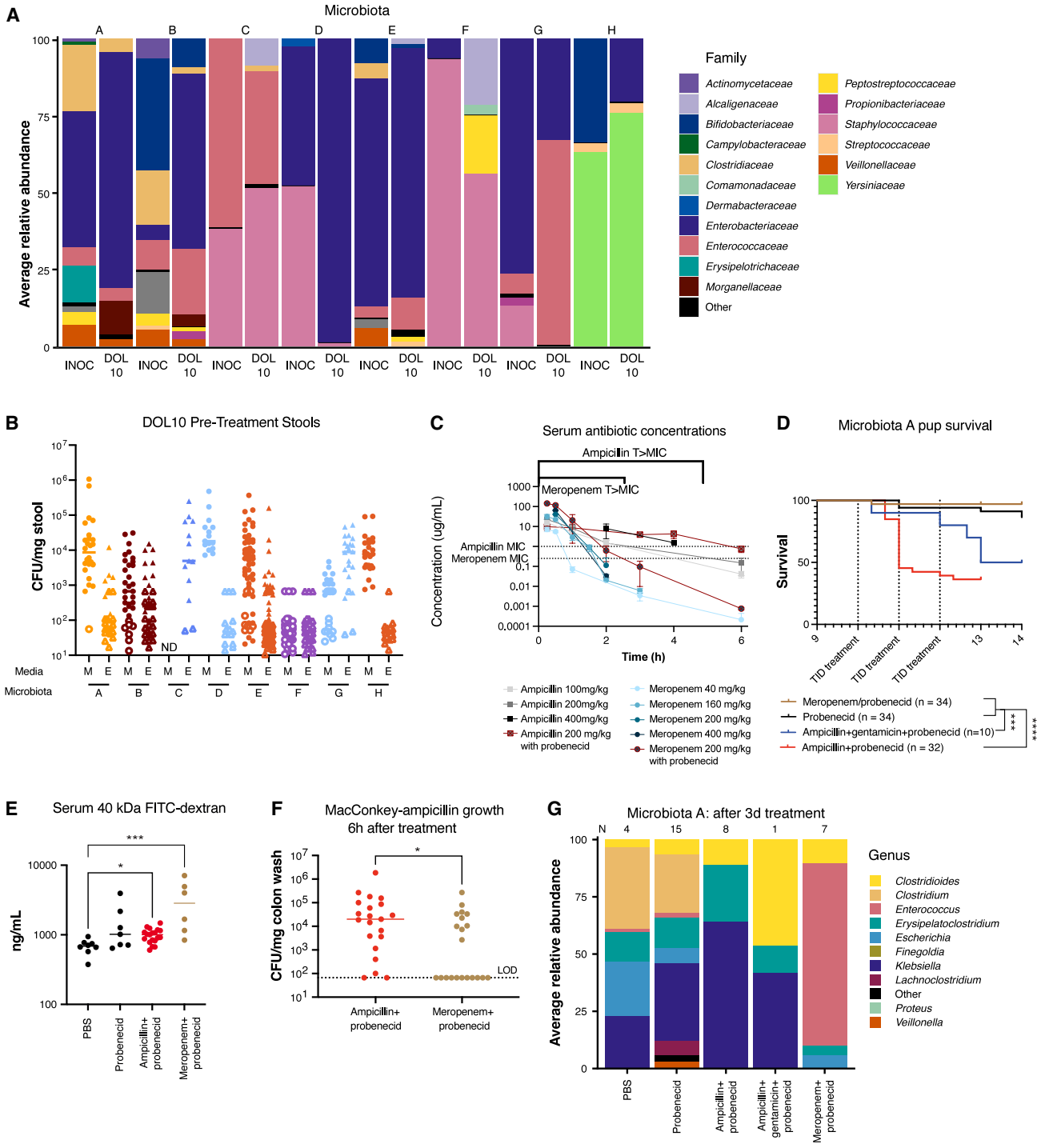


Figure 2. Establishment of representative microbiota humanization and pup antibiotic treatment outcomes

(A) Average relative abundance is plotted at the family level from stool from the human infant (INOC) and gnotobiotic mouse pups at DOL 10. Taxa with less than 1% relative abundance are pooled together into "Other." N = 1–5 experiments with n = 15–83 pups.

(B) CFUs/mg from pup stools at DOL 10 are plotted to MacConkey (M) and Enterococcosel (E) agar. KW with post hoc Dunn's multiple comparison statistics in Data S4. Samples with no detectable CFUs were set to the LOD based on individual stool weight and plotted as open shapes.

(C) Conventional mouse pups were injected subcutaneously with the listed antibiotic, and serum concentrations were determined with LC-MS at the indicated time points. N = 2–5 samples per antibiotic time point. Error bars represent standard deviation.

(legend continued on next page)

Please cite this article in press as: Schwartz et al., Microbiome-antibiotic-immune interactions influence mortality in preterm infant gut microbiota-humanized gnotobiotic mice, Cell Reports Medicine (2026), https://doi.org/10.1016/j.xcrm.2026.103161

measured serum concentrations with mass spectrometry (Figure 2C). Our goal was to identify dosing regimens approximating human preterm neonatal serum concentrations with a time above a minimum inhibitory concentration ($T_{>MIC}$) of 1 μg/mL ampicillin for 50% and $T_{>MIC}$ above 0.25 μg/mL meropenem for 40% of the dosing interval.[42–45] We found that probenecid, which inhibits renal excretion of β-lactams,[46] extended the half-lives of ampicillin and meropenem, resulting in a $T_{>MIC}$ of 70.0% for ampicillin (MIC of 1 μg/mL) and 36.3% for meropenem (MIC of 0.25 μg/mL) during an 8-h (q8h) dosing interval (Figure 2C; Data S4). Having established a dosing regimen, we determined the effects of specific antibiotics on microbiota-humanized pups.

Microbiota A-humanized mouse pups die during antibiotic treatment

Microbiota A-humanized pups treated q8h for 3 days with meropenem + probenecid or probenecid alone survived, whereas 50% and 72% of pups died during ampicillin + gentamicin + probenecid and ampicillin + probenecid treatments, respectively (Figure 2D; Data S4). One day post-treatment initiation, pups treated with meropenem + probenecid gained 5% average weight from baseline, whereas ampicillin + probenecid-treated and probenecid-treated pups lost 2.6% and 0.6% of weight on average, respectively (Figure S2A, $p = 0.002$). 13/14 (93%) animals that were found deceased, but intact, during ampicillin + probenecid treatment had culturable bacteria in their spleen (Figure S2B). Matrix-assisted laser desorption/ionization (MALDI) mass spectrometry on bacterial colonies from eight of these mice identified *Klebsiella* spp. and/or *E. coli* (Figure S2B). Because these genera were the most abundant within the gut before treatment (Figure 2A), we hypothesized that bacteria translocated into the bloodstream during ampicillin + probenecid treatment. To test this hypothesis, we orally gavaged 40-kDa fluorescein isothiocyanate (FITC)-dextran 2 h after antibiotic injection and quantified serum FITC-dextran 4 h later. We found increased serum 40-kDa FITC-dextran, indicating increased gut permeability, with both ampicillin + probenecid and meropenem + probenecid treatments compared to PBS (Figure 2E; Data S4). Microbiota A-humanized pups did not die during meropenem treatment but had evidence of increased gut permeability (Figures 2D and 2E). We hypothesized that meropenem effectively killed Gram-negative *Enterobacteriaceae* that instead disseminated during ampicillin + probenecid treatment. Indeed, 6 h after subcutaneous antibiotic injection, ampicillin-resistant Gram-negative bacterial titers in colon wash were lower in meropenem + probenecid- than in ampicillin + probenecid-treated pups ($p < 0.05$, Figure 2F). Further, in colons and stools, after 3 days of meropenem + probenecid treatment, the gut microbiota was dominated by 80% *Enterococcus* with 5% *Escherichia* and no *Klebsiella* (Figure 2G). Conversely, ampicillin-treated pups that survived treatment harbored 64% *Klebsiella* in the gut microbiome. Meropenem effectively reduced Gram-negative gut microbiota colonization during 3 days of q8h treatment (Figure S2C). After treatment on DOL 13, ampicillin-treated pups had increased β-lactam antibiotic resistance gene burden compared to meropenem-treated pups ($p = 0.02$, Figure S2D; Data S3). Thus, mortality in Microbiota A-humanized pups during ampicillin + probenecid treatment was associated with systemic dissemination, driven by increased gut permeability and antibiotic-dependent selection for Gram-negative *Enterobacteriaceae* (e.g., *Klebsiella*), in contrast to meropenem, which depleted Gram-negatives and favored *Enterococcus* predominance without dissemination.

Microbiota B-humanized pups die during meropenem + probenecid treatment

We observed minimal mortality in Microbiota A-humanized pups during meropenem + probenecid treatment. Because Microbiota B-humanized pups harbored a similar abundance of Gram-negative bacteria compared to Microbiota A-humanized pups (Figure 2A), we hypothesized that meropenem would also be protective in the Microbiota B background. We further hypothesized that killing Gram-positive competitors with vancomycin would lead to *Enterobacteriaceae* blooms. Surprisingly, Microbiota B-humanized mouse pups succumbed more frequently during meropenem + probenecid treatment (23 deaths/62 mice) than during vancomycin + probenecid treatment (6 deaths/47 mice) (Figure 3A, $p = 0.0325$). Animal weights during treatment did not significantly differ (Figure S3A). In animals found deceased and intact, we rarely documented bacterial dissemination (Figure S3B). Although we did not detect overt bacterial dissemination to systemic sites, we evaluated whether increased gut permeability could explain this lethality. We observed no differences between any treatments ($p > 0.05$) in 40-kDa FITC-dextran serum concentrations 6 h after subcutaneous injection (Figure 3B), unlike in Microbiota A-humanized pups. In summary, Microbiota B-humanized pups died during meropenem + probenecid treatment without obvious bacterial dissemination.

Because we observed discordant phenotypes between Microbiota A- and B-humanized pups during meropenem + probenecid treatment, we hypothesized that antibiotic + probenecid-microbiota interactions influenced outcome. To determine why Microbiota B-humanized pups succumbed during antibiotics, we compared stool and colon wash microbiota compositions during/after treatments between mice that died and survived (Figure 3C). We identified significant differences in microbiota composition associated with mortality using MaAsLin3.[47] Animals that survived had significantly decreased

(D) Survival of Microbiota A-humanized mouse pups subcutaneously injected q8h for 3 days starting at DOL 10. *p* values determined with pairwise log rank test with Benjamini-Hochberg (BH) correction. $N = 2–6$ experiments with $n = 10–34$ total mice per group.

(E) 40-kDa FITC-dextran was measured in serum 4 h after oral gavage and 6 h after subcutaneous injection of the listed agents. $^{*}p < 0.05$; $^{***}p < 0.005$, KW with post hoc Dunn's test, BH corrected.

(F) Growth of bacteria on MacConkey agar with ampicillin was enumerated 6 h after injection with the listed agents. $^{*}p < 0.05$, Mann-Whitney.

(G) Average relative abundance is plotted from fecal samples and colon washes after 3 days of q8h treatment with the listed agents. Number of mice per group is listed above the stacked bar plot.

Please cite this article in press as: Schwartz et al., Microbiome-antibiotic-immune interactions influence mortality in preterm infant gut microbiota-humanized gnotobiotic mice, Cell Reports Medicine (2026), https://doi.org/10.1016/j.xcrm.2026.103161

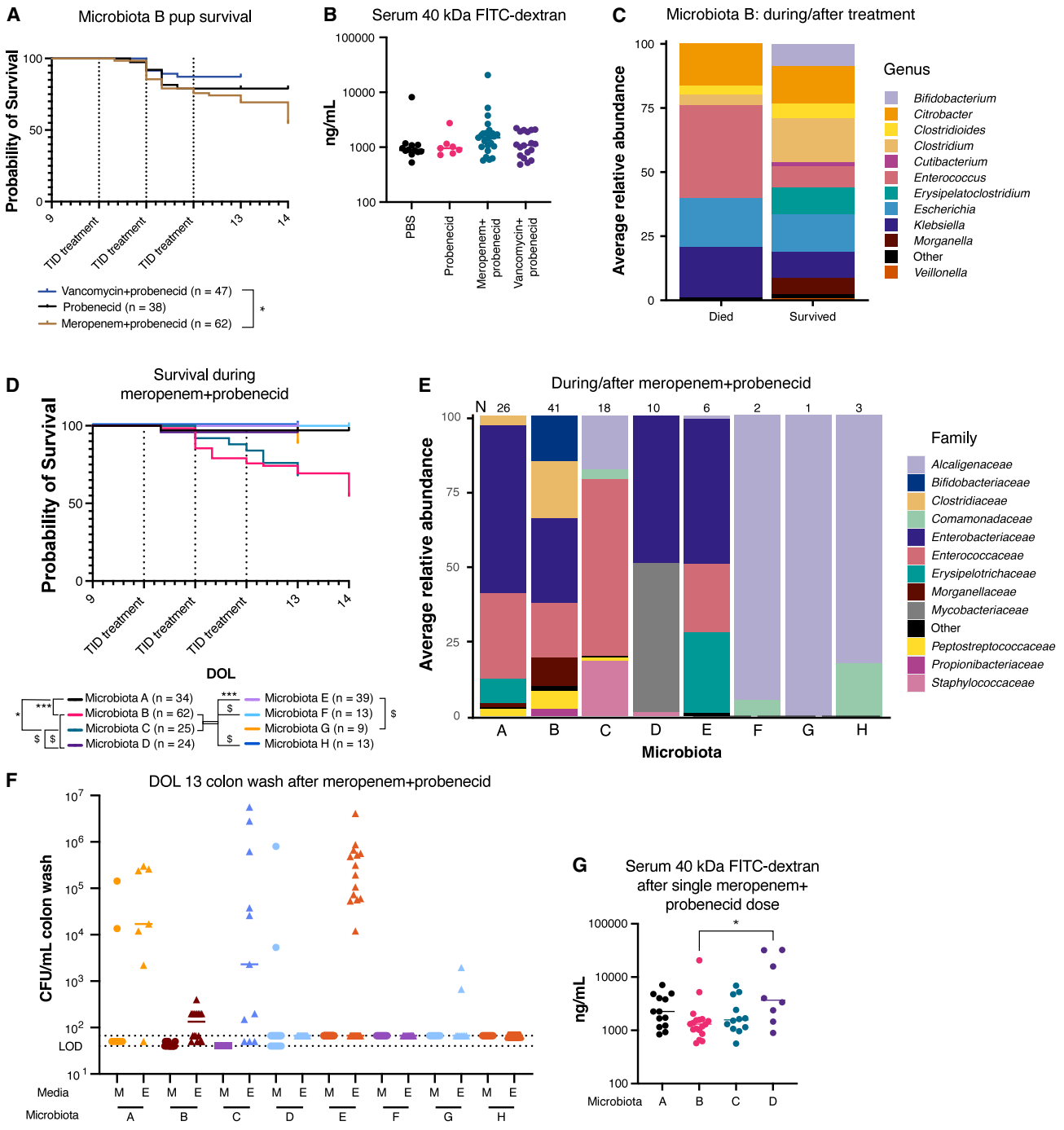


Figure 3. Survival of humanized mouse pups during antibiotic treatment correlates with microbiota composition

(A) Survival curves of Microbiota B-humanized mouse pups subcutaneously injected with the listed treatments q8h starting on DOL 10. *p* values determined with pairwise log rank test. *N* = 6–9 experiments with 38–62 total mice per group.

(B) Serum 40-kDa FITC-dextran was measured 4 h after oral gavage and 6 h after subcutaneous administration of the listed agents in Microbiota B-humanized pups.

(C) Average relative abundance is plotted at the genus level from stool and colon wash for Microbiota B-humanized pups that did or did not die during treatment. *N* = 12 samples from 11 mice that died (5 probenecid, 5 meropenem + probenecid, and 1 vancomycin + probenecid) and 99 samples from 115 mice that survived meropenem + probenecid, probenecid, and vancomycin + probenecid treatments.

(D) Survival is plotted during q8h meropenem + probenecid administered from DOL 10–13. *q* values determined with log rank (Mantel-Cox test) with BH correction in Data S4. $*q* < 0.1, *$*q* < 0.05, ***$*q* < 0.005; *N* = 1–9 experiments with 9–62 mice per group. Data for Microbiota A and B reproduced here from Figure 2D and (A).

(legend continued on next page)

Please cite this article in press as: Schwartz et al., Microbiome-antibiotic-immune interactions influence mortality in preterm infant gut microbiota-humanized gnotobiotic mice, Cell Reports Medicine (2026), https://doi.org/10.1016/j.xcrm.2026.103161

Enterococcus relative abundance with 8.5% versus 36% (Data S4, coeff. −2.3, $q = 0.03$). These results indicate that unlike Microbiota A, mortality in Microbiota B-humanized pups during antibiotic treatment was not explained by increased gut permeability or Gram-negative-mediated systemic dissemination. Rather, mortality was associated with antibiotic-induced changes in community composition, specifically *Enterococcus*.

Microbiota similarity correlates with outcome during antibiotic treatment

We hypothesized that gut *Enterococcus* abundance was associated with death during meropenem + probenecid treatment in Microbiota B-humanized pups. We tested this hypothesis with pups humanized with Microbiota G and C (67% and 37% *Enterococcus* abundance, respectively), Microbiota E and A (10% and 4% *Enterococcus*, respectively), and Microbiota D, F, and H (which lacked *Enterococcus*) (Figures 2A and 2B). Microbiota A-, D-, E-, F-, and H-humanized pups survived during meropenem + probenecid treatment (Figure 3D), whereas 32%–37% of Microbiota B- and C-humanized pups died during treatment ($q < 0.1$, Figure 3D; Data S4). 1/9 (11%) Microbiota G-humanized pups died, which was significantly greater than 0/39 (0%) Microbiota E-humanized pups ($q < 0.1$, BH-corrected log rank). Taken together, the three microbiota conditions with the greatest *Enterococcus* abundance at DOL 10 (B, C, G) were more likely to die with meropenem + probenecid treatment than animals with less than 10% abundance at baseline.

We next hypothesized that microbial changes during meropenem + probenecid treatment might correlate with death or survival. Gut microbiota of stool and/or colons of Microbiota A-humanized pups had relative decreases in *Enterobacteriaceae* from DOL 10 samples (77% to 55.5%) and increases in *Enterococcaceae* (4% to 29%) during and after meropenem + probenecid treatment (Figures 2A and 3E). Similarly, meropenem + probenecid decreased *Enterobacteriaceae* from 57% at DOL 10 to 28% at DOL 13 in Microbiota B-humanized pups. *Enterococcaceae* also expanded in Microbiota C-humanized pups from 37% to 59% and in Microbiota E-humanized pups from 10% to 23% (Figure 3E). Meropenem + probenecid eliminated most colonic bacteria in Microbiota F-, G-, and H-humanized pups as inferred by 26/32 samples (81%) failing sequencing with low microbial reads (Data S3). The remaining microbial reads (<3% of total reads) indicated *Alcaligenaceae* and *Comamonadaceae*, which was confirmed with absence of growth on MacConkey and Enterococcosel agar for 33/35 samples (Figure 3F). Colon washes from two Microbiota G-humanized mice had $\sim 10^3$ CFU/mL *Enterococcus* remaining after treatment. After meropenem + probenecid, *Enterococcus* CFUs in colonic contents were also increased relative to growth on MacConkey agar for Microbiota B ($p < 0.0005$) and C ($p < 0.05$) (Figure 3F; Data S4). Unlike *Enterobacteriaceae*, which have meropenem MIC breakpoints of 1 μg/mL, *E. faecalis* strains often have higher MICs of 4–8 μg/mL.[48,49] Indeed, the isolated *E. faecalis* from Microbiota A, B, and C had greater MICs (8, 8, and 4 μg/mL, respectively [Data S3]) than the meropenem-susceptible *Enterobacteriaceae* from these samples. Although we did not measure fecal meropenem concentrations, it is likely that the gut concentration of meropenem did not exceed 8 μg/mL for longer than an hour based on measured serum concentrations (Figure 2C).

We next pursued the association between increased DOL10 stool *Enterococcus* abundance and mortality during meropenem + probenecid treatment. We hypothesized that *Enterococcus* did not disseminate in Microbiota C-humanized mice like our observation in Microbiota B-humanized mice. Consistent with this hypothesis, we did not detect bacteria in the spleen or liver of Microbiota C-humanized pups (Figure S3C). Accordingly, Microbiota B- and C-humanized pups had the lowest serum 40-kDa FITC-dextran concentrations 6 h after a single meropenem + probenecid injection, demonstrating low gut permeability (Figure 3G). Probenecid, by itself, was not associated with increased gut permeability in Microbiota A-, B-, or C-humanized pups (Figure S3D). Microbiota B- and C-humanized pups did not demonstrate increased gut permeability with any of the tested regimens (Figure 3B; Figure S3E). These results suggest that mortality during meropenem + probenecid treatment was related to antibiotic-mediated *Enterococcus* enrichment and not gut permeability and systemic dissemination.

Microbiota similarity correlates with immune response during antibiotic + probenecid treatment

Because we did not observe overt bacterial dissemination with Microbiota B- and C-humanized pups that died during meropenem + probenecid treatment, we hypothesized that systemic immune dysregulation in response to gut microbiota alterations could be responsible. We measured serum concentrations of 23 cytokines 6 h after injection with either PBS or meropenem + probenecid and observed several patterns (Figure 4; Figure S4). First, we observed that meropenem + probenecid did not significantly alter serum cytokines in Microbiota A-humanized pups compared to PBS treatment ($p > 0.05$). G-CSF increased in Microbiota C-humanized pups ($p < 0.01$) and IL-1β ($p < 0.01$), IL-2 ($p < 0.05$), IL-4 ($p < 0.01$), IL-6 ($p < 0.05$), and IL-10 ($p < 0.05$) were increased in Microbiota B-humanized pups treated with meropenem + probenecid vs. PBS (Data S4, Kruskal-Wallis [KW] with post hoc Dunn's multiple comparison test). GM-CSF ($p < 0.005$), IL-12 (p40) ($p < 0.01$), MCP-1 ($p < 0.01$), and TNF-α ($p < 0.01$) were greater in Microbiota A-humanized pups at baseline (PBS treatment) vs. Microbiota C-humanized pups, which may reflect the absence of *Enterobacteriaceae* in the latter.[50,51] Similarly, Microbiota B-humanized

(E) Average relative abundance is plotted at the family level from stool and colon washes from pups during and immediately after meropenem + probenecid treatment. Taxa less than 1% average abundance are pooled to "Other." Sample number is listed above each stacked bar plot. $N = 1$–5 independent experiments.

(F) CFU/mL of colon wash is plotted from pups humanized with the listed microbiota and plated on MacConkey (M) or Enterococcosel (E) agar. Statistics in Data S4.

(G) 40-kDa FITC-dextran levels are plotted 4 h after oral gavage and 6 h after subcutaneous meropenem + probenecid injection to DOL 10 pups humanized with the listed microbiota. Statistical analysis with KW test with post hoc Dunn multiple hypothesis correction.

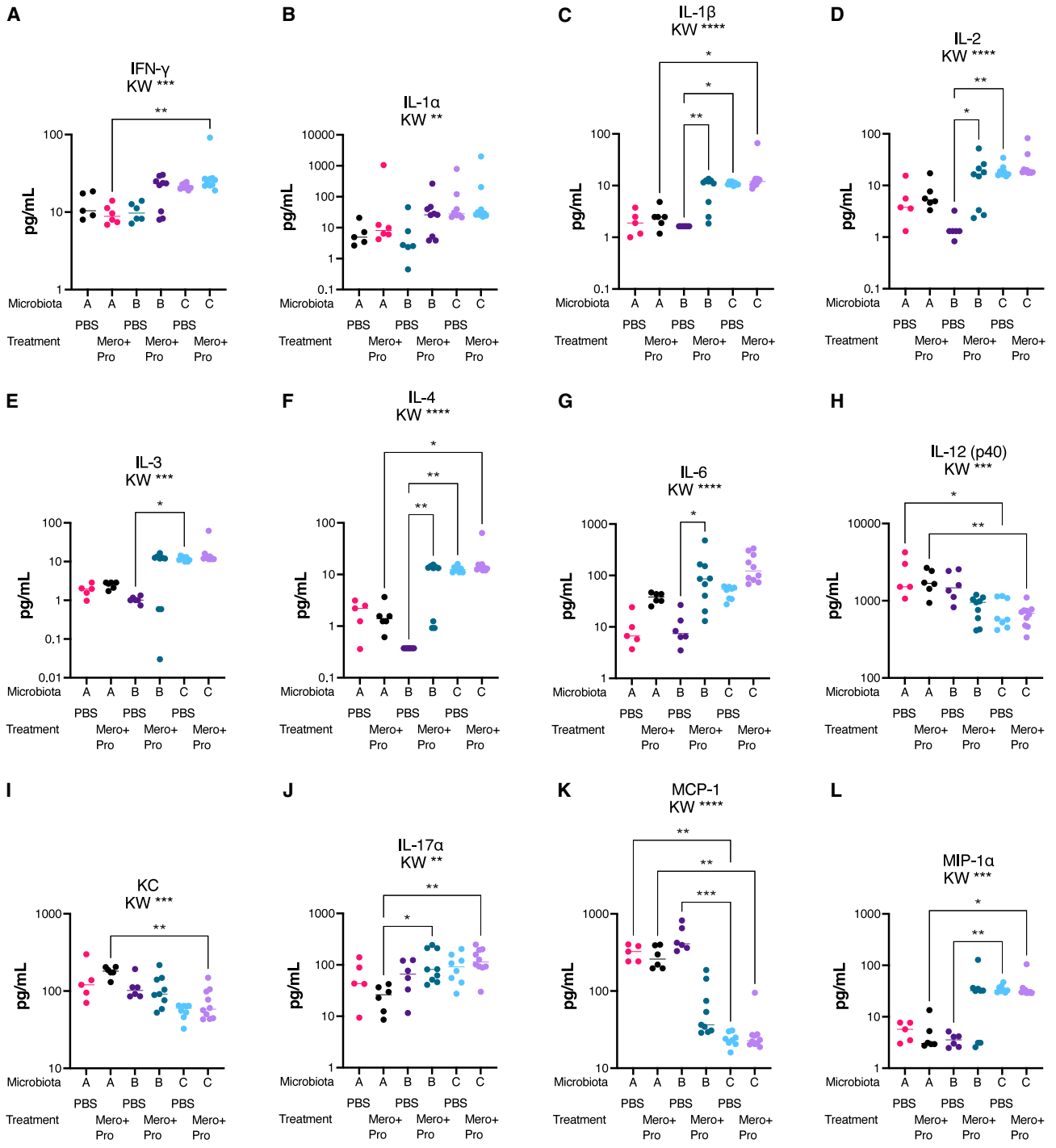


Figure 4. Systemic immune dysregulation in Microbiota B- and C-humanized mice treated with meropenem + probenecid

(A–L) Concentrations of 23 cytokines (remainder in Figure S4) were measured from the serum of DOL 10 pups 6 h after subcutaneous injection with PBS or meropenem + probenecid. Overall statistical analysis with KW test followed by pairwise Dunn's multiple hypothesis correction for each cytokine individually. *$p < 0.05$, **, $p < 0.01$, ***$p < 0.005$; ****$p < 0.001$.

pups had lower IL-1β ($p < 0.05$), IL-2 ($p < 0.01$), IL-3 ($p < 0.05$), IL-4 ($p < 0.01$), IL-9 ($p < 0.05$), and MIP-1α ($p < 0.01$) and increased MCP-1 ($p < 0.005$) compared to Microbiota C-humanized pups treated with PBS (Figure 4). Finally, Microbiota C-humanized pups treated with meropenem + probenecid had increased serum eotaxin ($p < 0.05$), IFN-γ ($p < 0.01$), IL-1β

Please cite this article in press as: Schwartz et al., Microbiome-antibiotic-immune interactions influence mortality in preterm infant gut microbiota-humanized gnotobiotic mice, Cell Reports Medicine (2026), https://doi.org/10.1016/j.xcrm.2026.103161

($p < 0.05$), IL-4 ($p < 0.05$), IL-5 ($p < 0.05$), IL-17α ($p < 0.01$), and MIP-1α ($p < 0.05$) and lower IL-12 (p40) ($p < 0.01$), KC ($p < 0.01$), and MCP-1 ($p < 0.01$) relative to Microbiota A-humanized pups. Collectively, we observed a trend where Microbiota B-humanized pups had intermediate cytokine profiles between the extreme responses of Microbiota A- and C-humanized pups.

In addition to prolonging the half-lives of β-lactam antibiotics,[46] probenecid inhibits pannexin channels, encoded by the *panx1* gene, abrogating ATP release in apoptotic cells.[52,53] Therefore, we investigated whether the combination of meropenem and probenecid altered *panx1* expression and if so, whether it differed between microbiota-humanized pups. We found that a single injection of meropenem + probenecid altered the expression of *panx1* in Microbiota B- and C-humanized mice compared to PBS (Wilcoxon $p < 0.01$ and $p < 0.05$, respectively), but in opposite directions (Figure S5A). Relative to other conditions, Microbiota B-humanized pups had significantly increased expression ($p < 0.05$ vs. A and $p < 0.005$ vs. C). Pannexin-1 is an upstream regulator of the inflammasome, leading to the release of IL-1β.[54–56] We observed the largest increase in *panx1* expression (Figure S5A) and serum IL-1β (Figure 4) in Microbiota B-humanized mice treated with meropenem + probenecid relative to PBS. These data suggest that in Microbiota B-humanized mice, death during meropenem + probenecid treatment is associated with increased IL-1β and *panx1* expression.

Overall, 21% (8/38) of Microbiota B-humanized mice died during probenecid treatment (Figure 3A). We observed minimal deaths during treatment of either Microbiota A- or Microbiota B-humanized pups when probenecid was omitted (Figure S5B). Probenecid-containing regimens did not cause death in germ-free pups, suggesting that this phenotype required microbial colonization (Figure S5C). Similarly, conventional specific-pathogen free mice did not succumb during probenecid-containing regimens (Figure S5D). Because of our data above demonstrating variable death depending on microbiota composition, we hypothesized that probenecid could have effects specifically on the immune system of preterm microbiota-humanized pups. We observed no statistically significant increases in mortality with Microbiota A- to E-humanized pups treated with probenecid (Figure S5E, log rank $p > 0.05$). However, like Microbiota B-humanized mice, 40% (6/15) of Microbiota C-humanized mice died during probenecid treatment. Meropenem + probenecid treatment was not statistically increased above probenecid alone (Data S4), suggesting probenecid could be immune-modulatory and associated with the phenotype. We did not observe significant associations between DOL 10 gut microbiome composition and death during probenecid (Data S4). Nevertheless, we explored whether probenecid might have immune effects because of increased mortality of Microbiota B- and C-humanized pups compared to Microbiota A-humanized, germ-free, and conventional pups.

We subcutaneously injected 200 mg/kg probenecid to Microbiota A-, C-, and conventional mouse pups and measured serum cytokines 6 h later. We found increased eotaxin, IFN-γ, IL-1α, IL-1β, IL-2, IL-3, IL-4, IL-5, IL-6, IL-17α, and MIP-1α and decreased G-CSF, GM-CSF, IL-10, IL-12 (p40), and MCP-1 in Microbiota C-humanized pups relative to Microbiota A-humanized and/or conventional pups (Figure S6; Data S4). Although many cytokine differences are present at baseline (Figure 4; Data S4), these data suggested differential impacts of probenecid depending on colonizing microbes. To further explore this phenotype, we compared serum cytokines after 3 days of q8h treatments of probenecid-containing and probenecid-lacking regimens in Microbiota A- and B-humanized pups. Compared to PBS, probenecid led to decreased IL-9, IL-12(p40), IL-17α, and RANTES for Microbiota A (Figure S7; Data S4, KW < 0.05 followed by post hoc Dunn's test). However, 3 days of q8h ampicillin + probenecid, a regimen leading to death in Microbiota A-humanized pups (Figure 2D), led to decreased G-CSF, IL-10, and KC and increased IL-2 relative to probenecid alone (Figure S7; Data S4). Furthermore, numerous cytokines including IL-1α, IL-1β, IL-2, IL-3, IL-4, and MIP-1α were elevated in Microbiota A-humanized pups treated with ampicillin + probenecid vs. meropenem + probenecid, suggesting persistent immune dysregulation in the absence of overt mortality. Similarly, 3 days of meropenem + probenecid, which was associated with death in Microbiota B-humanized pups, led to decreased IFN-γ, IL-1α, IL-1β, IL-2, IL-3, IL-4, IL-6, and MIP-1α and increased MCP-1 relative to probenecid only (Figure S8; Data S4, KW < 0.05 followed by post hoc Dunn's test). These data confirm that while probenecid affects the immune system depending on the infant microbiome present, antibiotics plus probenecid have further effects on immune responses.

Colonizing *E. faecalis* strains differ in their virulence repertoire

Microbiota A, B, C, E, and G contain *Enterococcus faecalis*, yet only pups humanized with Microbiota B, C, and G succumbed during probenecid and/or meropenem + probenecid treatment. We hypothesized that differences in virulence factors between these *E. faecalis* strains could contribute to the different outcomes. We cultured the human stool inoculum on Enterococcosel agar and performed whole-genome sequencing of the resulting *E. faecalis* isolates (Data S3). Whole-genome assemblies were mapped to the Virulence Factor database (VFDB) to determine virulence factor presence.[57] One pair of virulence factors of particular interest was gelatinase, encoded by *gelE*, and the *Fsr* quorum sensing system, encoded by the *fsr* locus. *E. faecalis* from Microbiota B, C, and G encoded both the full *fsr* locus and *gelE*, while *E. faecalis* from Microbiota A and E encoded *gelE* but lacked *fsrA* and *fsrB* (Data S3). Indeed, *E. faecalis* isolated from Microbiota B, C, and G were positive for gelatinase activity (Gel+), while *E. faecalis* isolated from Microbiota A and E were Gel− (Data S3). *E. faecalis* gelatinase cleaves pro-IL-1β into mature IL-1β,[58] and previous work has shown that *gelE* is regulated by the *Fsr* quorum sensing system.[59] We observed increased serum IL-1β in pups colonized with Microbiota B and C and treated with meropenem + probenecid relative to Microbiota A-humanized pups (Figure 4). Thus, strain-specific differences in same-species colonization were associated with immune response and mortality during meropenem + probenecid treatment.

Please cite this article in press as: Schwartz et al., Microbiome-antibiotic-immune interactions influence mortality in preterm infant gut microbiota-humanized gnotobiotic mice, Cell Reports Medicine (2026), https://doi.org/10.1016/j.xcrm.2026.103161

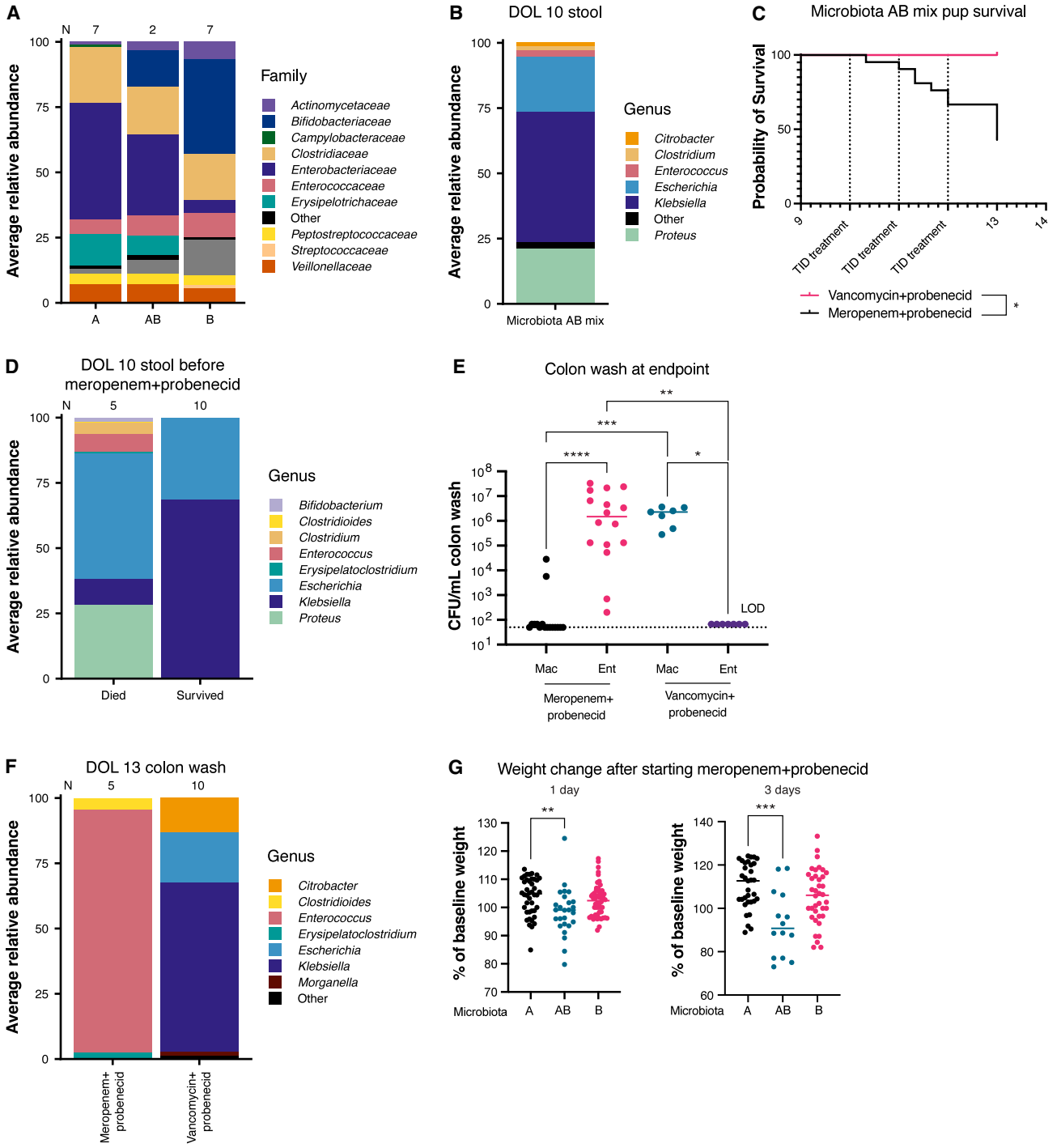


Figure 5. Microbiota AB-mix results in animal death during meropenem + probenecid treatment with concomitant *Enterococcus* expansion

(A) Average relative abundance at the family level. *N* = 7 samples for Microbiota A and B; *N* = 2 samples for Microbiota AB-mix.

(B) Average relative abundance at the genus level of fecal samples from pups on DOL 10. *N* = 24 samples from 2 independent experiments.

(C) Survival of Microbiota AB-humanized pups during q8h treatment. *N* = 1–2 experiments with 7–21 total mice. $^{*}p < 0.05$ log rank.

(D) Average relative abundance of fecal samples on DOL 10 stratified by whether they died or survived during 3 days of q8h meropenem + probenecid treatment.

(E) CFUs/mL of colon contents plated on MacConkey and Enterococcosel agar. LOD, limit of detection.

(legend continued on next page)

Please cite this article in press as: Schwartz et al., Microbiome-antibiotic-immune interactions influence mortality in preterm infant gut microbiota-humanized gnotobiotic mice, Cell Reports Medicine (2026), https://doi.org/10.1016/j.xcrm.2026.103161

CellPress
OPEN ACCESS

Mixed Microbiota A- and B-humanized mice succumb during meropenem + probenecid treatment

Treatment with broad-spectrum antibiotics like meropenem, is associated with microbiota shifts with *Enterococcus* and *Enterobacteriaceae* frequently colonizing and persisting within an infant's gut microbiota where they were previously absent.[6] Further, microbiota shift events during antibiotic treatment are associated with dramatic changes in relative abundance of commensals and potential pathogens.[6,11] To determine if Microbiota A had protective species or Microbiota B harbored dominant pathogenic species important for immune dysregulation and death during meropenem + probenecid, we combined fecal samples prior to introduction into pregnant dams to create a Microbiota AB-mixed community.

The four most abundant families in the Microbiota AB-mixed inocula were *Enterobacteriaceae* (31%), *Clostridiaceae* (18%), *Bifidobacteriaceae* (14%), and *Enterococcaceae* (8%), reflecting a balance between Microbiota A and B individual inocula (Figure 5A). At DOL 10, the gut microbiota of AB-humanized mice was dominated by *Enterobacteriaceae* including 50% *Klebsiella* and 21% *E. coli* (Figure 5B) like Microbiota A- and B-humanized pups (Figure 2A). Stool contained a median of 4×10^3 CFUs/mg Gram-negative organisms grown on MacConkey agar and 7.5×10^1 CFUs/mg *Enterococcus* ($p < 0.001$; Figure S9A). Like Microbiota A- and B-humanized pups, individual fecal samples harbored a wide range of abundances of *Enterobacteriaceae* and *Enterococcaceae*. Individual fecal samples from Microbiota AB-humanized pups at DOL 10 variably resembled microbiota from Microbiota A- or B-humanized pups when visualized by PCoA (Figure S9B). There were no significant overall differences by colonizing microbiota (Figure S9B, PERMANOVA $p > 0.05$). However, we observed greater compositional differences in PCO1 and PCO2 between Microbiota A- and B-humanized pups ($p < 0.005$) than between Microbiota AB-humanized pups and either Microbiota A- or B-humanized pups. Therefore, Microbiota AB-humanized mice have similarities to both Microbiota A- and B-humanized pups, representing an intermediate composition of both.

At DOL 10, we treated Microbiota AB-humanized pups with subcutaneous antibiotics as before. 12/21 (57%) pups died during meropenem + probenecid treatment relative to 0/7 (0%) treated with vancomycin + probenecid ($p < 0.05$, Figure 5C). Pups that survived during meropenem + probenecid treatment harbored almost exclusively *Klebsiella* and *Escherichia* (99.7%) in stool on DOL 10 before treatment (Figure 5D). Pups that died during meropenem + probenecid treatment also had high abundance of Gram-negative *Klebsiella*, *Proteus*, and *Escherichia* (86%), but they also harbored *Enterococcus* (7%) and other organisms (Figure 5D). At the experiment endpoint of DOL 13 or in animals discovered deceased, but intact, during treatment, meropenem + probenecid effectively eliminated Gram-negative colonic bacteria (Figure 5E). Conversely, colon washes contained 1.5×10^6 CFU *E. faecalis*, which was eliminated in animals treated with vancomycin + probenecid ($p < 0.01$, Figure 5E). Consistent with this finding, the gut microbiota after meropenem + probenecid treatment was 93% *Enterococcus* on average vs. nearly absent (0.14%) in pups treated with vancomycin + probenecid (Figure 5F). Thus, we observed a correlation between high *E. faecalis* abundance before and during treatment with death during meropenem + probenecid, which was rescued by vancomycin + probenecid treatment.

Because pups humanized with Microbiota AB-mixed inocula died during meropenem + probenecid treatment, we hypothesized that their immune responses would resemble those elicited in Microbiota B-humanized animals (Figure 4). We also hypothesized that animals surviving to the treatment endpoint would have inflammatory signatures distinct from Microbiota A-humanized pups, which nearly universally survived during meropenem treatment. Among statistically significant cytokines, we found that pups humanized with Microbiota AB-mix demonstrated similar cytokine responses to pups humanized with Microbiota B after 3 days of q8h treatment (Figure S10). Specifically, Microbiota B- and AB-humanized pups had lower GM-CSF, IFN-γ, IL-10, IL-13, and TNF-α compared to Microbiota A-humanized pups (Figure S10; Data S4). Microbiota AB-humanized pups lost significantly more weight than Microbiota A-humanized pups 1 day into treatment (Figure 5G, left; $p < 0.01$) and at the conclusion of the experiment (Figure 5G, right; $p < 0.005$). Collectively, these data suggest that the blunted immune response during treatment is not protective, resulting in increased weight loss and mortality.

Recent meropenem exposure alters serum cytokine responses and increases *E. faecalis* abundance in preterm neonates

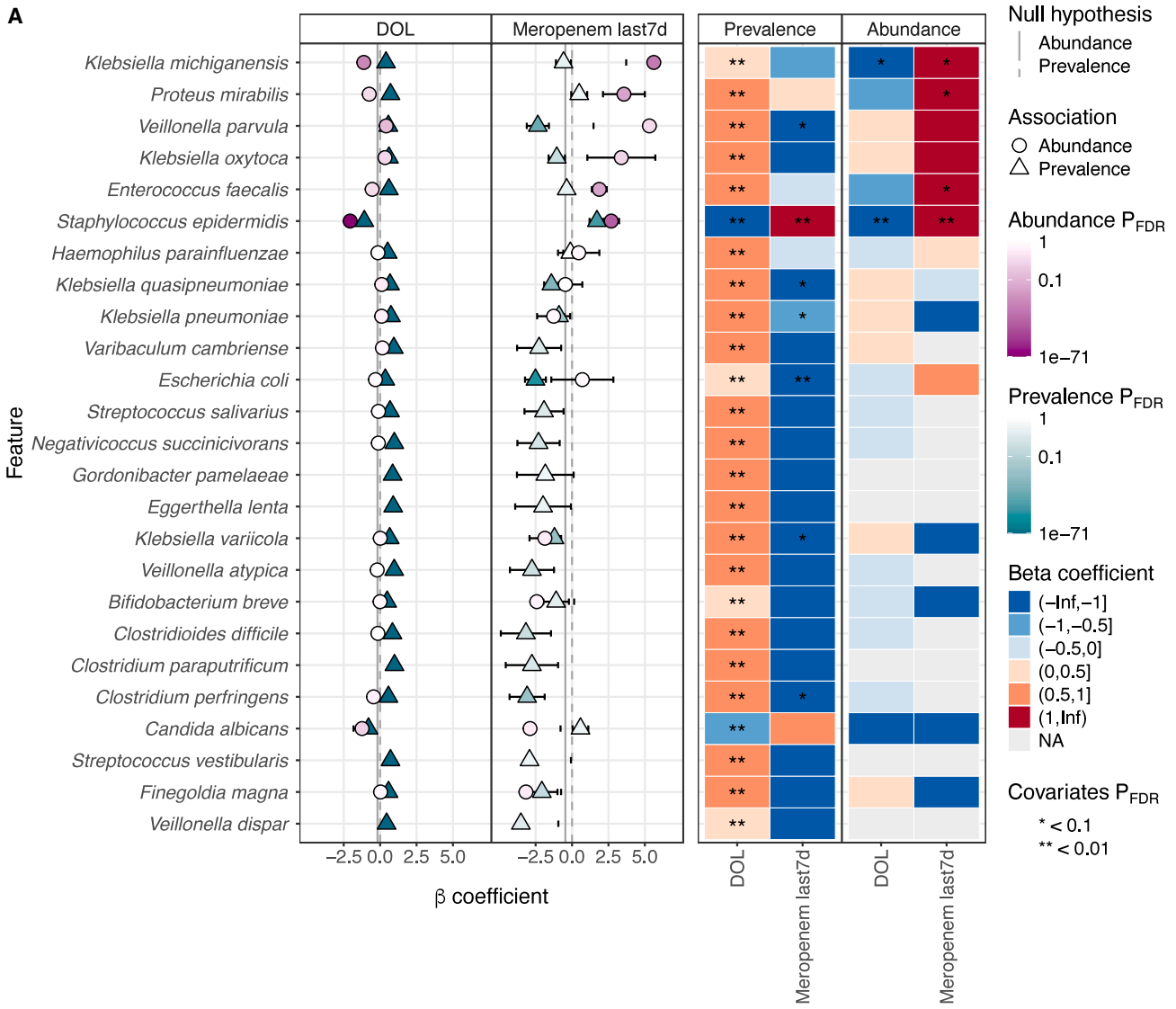
Cytokines including IL-10, IFN-γ, IL-1, IL-17, and IL-6 have been associated with LOS, microbiome composition, and antibiotic treatment in human preterm infants.[60–62] We observed changes in these cytokines in our gnotobiotic mouse model depending on the microbiome and antibiotic combination. Although mortality among preterm infants in the United States is 20%–30%,[63] only 78/977 (8%) expired during our study. We therefore did not have the power to associate meropenem receipt with infant death. However, to determine if similar inflammatory changes that we observed in mice occurred in human infants, we measured 37 cytokines in plasma collected 10 days prior to meropenem and compared them to samples collected up to 7 days after meropenem in the same 12 infants (Data S4). Most cytokines did not appreciably change; however, IL-10, IL-32, and IL-34 decreased 6- to 10-fold after meropenem (Figure S11, $p < 0.1$, Data S4). Importantly, IL-32 and IL-34 are both involved in IL-1 signaling,[64,65] which we observed in our animal model. Of these 12 infants, 9 (75%) did not have a positive bacterial culture and the other 3 had bacterial tracheitis (Data S4). Thus,

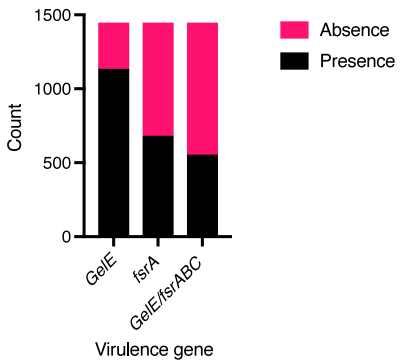
(F) Average relative abundance in DOL 13 colon washes after treatment with meropenem + probenecid or vancomycin + probenecid. $N = 1–2$ experiments with 5–7 mice each. Taxa below 1% average relative abundance are pooled together to "Other."

(G) Weight change 1 day and 3 days after meropenem + probenecid relative to baseline pre-antibiotic weight is plotted by microbiota. Animals that died before being weighed are not included; however, animals that met experimental endpoint criteria are. KW with post hoc Dunn's correction.

*$p < 0.05$, **$p < 0.01$, ***$p < 0.005$, ****$p < 0.001$.

Please cite this article in press as: Schwartz et al., Microbiome-antibiotic-immune interactions influence mortality in preterm infant gut microbiota-humanized gnotobiotic mice, Cell Reports Medicine (2026), https://doi.org/10.1016/j.xcrm.2026.103161





C

Meropenem in last day	p=0.0065	geIE/fsrABC present	geIE/fsrABC absent
	Yes	21	13
	No	529	880

Meropenem in last 3 days	p=0.0965	geIE/fsrABC present	geIE/fsrABC absent
	Yes	24	24
	No	526	869

Meropenem in last 7 days	p=0.3859	geIE/fsrABC present	geIE/fsrABC absent
	Yes	31	41
	No	519	852

Figure 6. *Enterococcus faecalis* containing key virulence factors is enriched in human preterm infants after meropenem

(A) Coefficient of change and Benjamini-Hochberg-corrected *q* value is displayed for the top 25 most significant associations between human gut microbiota species, DOL, and meropenem exposure in the last 7 days. Gestational age, delivery mode, fraction of days NPO, fraction of days of human milk, fraction of days

(legend continued on next page)

Please cite this article in press as: Schwartz et al., Microbiome-antibiotic-immune interactions influence mortality in preterm infant gut microbiota-humanized gnotobiotic mice, Cell Reports Medicine (2026), https://doi.org/10.1016/j.xcrm.2026.103161

meropenem was largely administered for culture-negative sepsis. While we cannot conclude whether the observed changes in IL-10, IL-32, and IL-34 were positive, neutral, or negative, these data suggest that meropenem can alter systemic immune responses in human preterm infants.

E. faecalis is one of the most abundant and prevalent members of the hospitalized preterm infant gut microbiota, colonizing greater than 60% of infants often at >50% abundance.[5–7,11,66] Antibiotic exposure, especially with broad-spectrum agents such as meropenem, has been associated with taxonomic changes, including expansion of *Enterococcus* in the infants' guts where it was previously undetected.[6,7,11] Identical strains of *E. faecalis*, ultimately identified in blood, increased in gut abundance in the 5–10 days prior to sepsis.[7] We wondered if recent meropenem exposure altered the abundance and prevalence of bacteria within the gut microbiota, including *E. faecalis*. We generated metagenomic profiles for 3,089 previously sequenced fecal samples from 266 hospitalized preterm infants (Data S1 and S2).[6,7,11,39] We determined microbiota associations with DOL; meropenem exposure in the 1, 3, and 7 days prior to fecal sampling; gestational age; delivery mode; fraction of days without oral nutrition (NPO) or with human milk or formula; and final disposition, controlling for individual, with MaAsLin3.[47] DOL was associated with small changes of key taxa in early life, including decreases in 5 *Staphylococcus* spp., as has been previously demonstrated[5,6] (Figure 6A; Data S4). Meropenem administration in the 7 days before fecal sampling dramatically decreased the abundance of anaerobes and Gram-negative bacteria consistent with its spectrum of activity[49] (Data S4). The abundance of species that exploit microbiota shifts,[6] including *S. epidermidis* and *E. faecalis*, increased after meropenem exposure (coef. 2.7 and 1.9, respectively, $q < 0.1$). Thus, we observed increases in *E. faecalis* in the gut microbiota after meropenem in our gnotobiotic mouse model and in human infants.

Because *E. faecalis* exploits available niches in the preterm infant gut microbiota, we evaluated the virulence factor repertoire of gut microbiota-colonizing strains. We generated 1,443 medium- and high-quality *E. faecalis* metagenomic-assembled genomes (MAGs) from 186 preterm infants from previously sequenced fecal samples from the same cohort.[6,7,11,39] We specifically focused on the *gel* and *fsr* loci, given our discordant observations in Microbiota A, B, C, E, and G and their implication in pathogenesis in other models.[58,67,68] 78% (1,127/1,443) of *E. faecalis* MAGs encoded *gelE*, while only 47% (676/1,439) encoded *fsrA* (Figure 6B; Data S5). 38% (549/1,439) of *E. faecalis* MAGs encoded the full *fsr* locus and *gelE* (Figure 6B; Data S5), which is similar to the *E. faecalis* isolated from Microbiota B, C, and G (Data S3). We then asked if colonizing strains differed in their virulence repertoire after meropenem exposure in human infants (Data S6). *E. faecalis* MAGs possessing the full *fsr* operon and *gelE* were over-represented in fecal samples 1 day after meropenem exposure (Figure 6C, $p = 0.0065$). Presence of these virulence factors in *E. faecalis* MAGs 3 and 7 days after meropenem was not statistically different ($p > 0.05$). These data suggest that the presence of these genes may confer a benefit in immediate *Enterococcus* gut repopulation or expansion after antibiotics. It has been previously observed that these virulence factors are more common in *E. faecalis* strains isolated from blood compared to gut colonization.[67] Conversely, other studies have associated *fsr* and *gelE* inactivation with increased biofilm formation, endocarditis, and bacteremia duration.[58,69] Thus, meropenem exposure enriches for *E. faecalis* gut colonization in human preterm neonates, including of strains with more virulence capacity after antibiotic-mediated disruption.

DISCUSSION

The gut microbiota of hospitalized preterm infants develops slowly and is frequently dominated by few species.[5–7,11] Antibiotics are administered to >80% of extremely-low-birthweight infants for suspected or confirmed bacterial infection.[4,10,70] Empiric antibiotic choices differ by NICU and geography[40] with β-lactams and aminoglycosides commonly co-administered.[35,71] Nevertheless, considerable heterogeneity in prescribing practices exists, and broad-spectrum agents, such as carbapenems, are administered empirically depending on the NICU.[35,71,72] Prolonged and unnecessary antibiotic receipt is associated with future risk of sepsis, gut microbiota disruption, and death in some cohorts.[12,13,15–17,73] Antibiotic interactions with the human host and gut microbiota are complex and multifaceted.

We developed a gnotobiotic mouse model of human neonatal gut microbiota development and antibiotic-mediated disruption to study these interactions. With eight representative microbiota, we found that certain pup microbiota-antibiotic combinations with probenecid resulted in death with evidence of systemic bacterial spread (culture-positive sepsis); death without bacterial dissemination, but with immune dysregulation (culture-negative sepsis); or microbiota disruption without mortality. Our model can therefore recapitulate observations in the NICU of variable outcomes during and after antibiotic treatment.[12,15,17] Specifically, we were able to model the clinical observation that continued antibiotics in the absence of a positive bacterial infection can be associated with immune dysregulation and mortality.[16]

Empiric treatment with an agent to which a potential pathogen in the gut was resistant resulted in dissemination and death. These data suggest that knowledge of the gut microbiota and resistome composition could inform empiric antimicrobial administration. Indeed, proof-of-principle work demonstrated that rapid long-read sequencing of the gut microbiota could more quickly inform empiric antibiotics for resistant potential pathogens in as little as 6 h.[74] In Microbiota AB-mix-, B-, C-, and G-humanized mice, we observed death during meropenem + probenecid

of formula, and final disposition were included as additional fixed effects, and individual was included as a random effect. Metadata, species taxonomy, and full list of significant taxa included in Data S1, S2, and S4. Error bars represent standard error of the coefficient.

(B) Number of medium- and high-quality *E. faecalis* MAGs containing the listed virulence factors are displayed.

(C) Association between *E. faecalis* MAG virulence gene presence and meropenem exposure from the infant from whom the fecal sample was collected in the prior 1, 3, or 7 days. Full list and metadata included in Data S5 and S6. *p* values determined with Fisher's exact test.

Please cite this article in press as: Schwartz et al., Microbiome-antibiotic-immune interactions influence mortality in preterm infant gut microbiota-humanized gnotobiotic mice, Cell Reports Medicine (2026), https://doi.org/10.1016/j.xcrm.2026.103161

treatment with *E. faecalis* expansion. Mixing Microbiota A and B prior to gavage demonstrated a lack of a protective feature in Microbiota A. Instead, we observed a dominant phenotype conferred by Microbiota B. We correlated these phenotypes to differences in the virulence factors *fsr* and *gelE* among *E. faecalis* within the gut microbiota. Future work with monocolonizations and genetic manipulation of these loci will be necessary to confirm and extend these associations.

In preterm infants, *E. faecalis* containing *fsr* and *gelE* were more likely to increase in abundance immediately after meropenem. These virulence factors contribute to biofilm formation, resistance to immune-mediated killing, and antibiotic resistance.[58,67,75] Further, gelatinase leads to increased gut permeability and *E. faecalis* translocation in cell culture models.[76,77] We did not detect overt bacterial dissemination, but it is possible that bacterial products leading to immune activation could explain animal mortality.[78] Although we achieved serum meropenem concentrations above the MIC for these *E. faecalis* strains, we do not know the gut meropenem concentration. In dosing trials of meropenem in preterm infants, meropenem did not lead to increased mortality over standard-of-care antibiotics.[41] However, our data here are consistent with prior observations that meropenem increases the gut abundance of *E. faecalis* and *S. epidermidis*.[11] Thus, careful consideration of antibiotic effects on gut microbiota composition should be incorporated into the clinical framework when deciding empiric antimicrobials for sepsis.

Ultimately, our goal is to limit unnecessary antibiotic treatment and prevent sepsis entirely. Therefore, optimizing early-life gut microbiota and immune development is key. Restricting gut microbiota development can lead to long-term infectious and immune consequences.[19,79] Preterm infants with the lowest gut microbiota Shannon diversity had persistent systemic changes in immune cells and proteins relative to term and preterm infants with more diverse gut microbiota.[19] These infants also had the highest inter-individual variance in immune development,[19] suggesting that understanding and optimizing the precise order of early-life microbial dynamics[5] could help inform long-term prognosis. Beneficial interventions like breastfeeding and breastmilk exposure have demonstrated consistent benefit through bioactive compounds such as immunoglobulins, beneficial microbes, and epidermal growth factor (EGF).[80–84] Similarly, probiotic supplementation can improve infant gut microbiota and immune development.[62,85,86] However, probiotic strains can be shared among untreated infants and have been implicated in causing sepsis,[85,87] so extreme caution is warranted when considering their administration.[88] Consideration of the effects of each medication and intervention on the gut microbiota and immune development will be essential for accurately predicting which infants are at risk of sepsis.[6,7,89]

Limitations of the study

Pups are born microbiota humanized, but dams were reared germ free prior to microbial colonization. Thus, an important limitation in our model is the lack of lifelong microbial exposure, which affects dam immune development, including the composition of breastmilk antibodies.[90] Similarly, the variability in dam colonization efficiency and time could impact the development of beneficial immune defenses. Although we used microbiota compositions representative of hospitalized preterm neonates worldwide,[5,6,8,62,85] strain-specific differences within species may not allow for our findings to be completely generalizable. Indeed, some of the observations in our mouse model could reflect exceptionally virulent strains. Similarly, our model required the addition of probenecid, which is not typically administered to preterm neonates. Despite this, diet, non-antibiotic medications, and the diseases for which they are prescribed alter the gut microbiome and gut permeability.[6,91,92] Accordingly, these findings will need to be validated and extended in other cohorts and with further mechanistic dissection in animal models.

RESOURCE AVAILABILITY

Lead contact

Further information and resource requests and reagents should be directed to the lead contact, Gautam Dantas (dantas@wustl.edu).

Materials availability

This study did not generate new unique reagents.

Data and code availability

- Processed shotgun metagenomic sequencing reads, whole-genome assemblies, and MAGs have been deposited in the NCBI BioProject PRJNA1402348 and are publicly available as of the date of publication. Accession numbers are listed in the key resources table.
- Custom code and primary data files have been deposited at https://github.com/DJSchwartzLab/NICUmousemodel (https://doi.org/10.5281/zenodo.23070073) and are publicly available as of the date of publication.
- Additional information required to reanalyze the data is the available from the lead contact upon request.

ACKNOWLEDGMENTS

The authors would like to thank the members of the Dantas lab, especially Robert Thänert and Skye Fishbein, for their experimental advice. We would also like to acknowledge the staff of the Edison Family Center for Genome Sciences and Systems Biology, including Eric Martin, Brian Koebbe, MariaLynn Crosby, and Jessica Hoisington-Lopez. The Genome Technology Access Center at the McDonnell Genome Institute, where sequencing was performed, is partially supported by the NCI Cancer Center Support Grant P30 CA91842 to the Siteman Cancer Center from the National Center for Research Resources (NCRR), a component of the National Institutes of Health (NIH), and NIH Roadmap for Medical Research. LC-MS analyses were supported by CDC 75D30121C11929 (J.P.H.). We would like to acknowledge the WashU Gnotobiotic Research, Education and Transgenic core (development supported by NIH C06OD028306) for support of and assistance with gnotobiotic experiments, including Summer Rucknagel, Sian Madden, and Mike White. We would like to thank Timari Bailey for assistance with gelatinase assays and Kevin Blake for figure editing. This research was supported by NIH grants K08 KAI159384 (D.J.S), R56HD116904 (D.J.S.), R01AI155893 (G.D.), CDC BAA OADS-1 (G.D.), UH3AI083265 (P.I.T.), and Washington University Digestive Diseases Research Core Center (P30 DK052574, Biobank Core, to co-director P.I.T.). This work was further supported by a Pediatric Infectious Diseases Society St. Jude Children's Hospital Fellowship in Basic and Translational Research (D.J.S.).

AUTHOR CONTRIBUTIONS

Conceptualization, D.J.S. and G.D.; methodology, D.J.S., G.G.W., K.E.W., T.S.C., J.I.R., and J.P.H.; analysis, D.J.S., G.G.W., K.E.W., I.R.E., J.T., N.S., and J.I.R.; investigation, D.J.S., G.G.W., K.E.W., I.R.E., J.T., J.N., L.Z.,

Please cite this article in press as: Schwartz et al., Microbiome-antibiotic-immune interactions influence mortality in preterm infant gut microbiota-humanized gnotobiotic mice, Cell Reports Medicine (2026), https://doi.org/10.1016/j.xcrm.2026.103161

A.W.D., A.F., T.S.C., M.A.W., and J.I.R.; resources, C.H.-M., R.B.S., M.A.W., J.P.H., C.-A.D.B., B.B.W., and P.I.T.; writing – original draft, D.J.S.; writing – review and editing, all authors; supervision, D.J.S., B.B.W., P.I.T., and G.D.; funding acquisition: D.J.S. and G.D.

DECLARATION OF INTERESTS

P.I.T. is a holder of equity in, a consultant to, and a member of the Scientific Advisory Board of MediBeacon Inc., which is developing a technology to non-invasively measure intestinal permeability in humans. P.I.T. is a co-inventor on patents assigned to MediBeacon (US patents 11,285,223 and 11,285,224 titled "Compositions and methods for assessing gut function" and US patent application 2022-0326255, "Methods of monitoring mucosal healing"), which might earn royalties if the technology is commercialized. He is a member of the Data Safety Monitoring Board of Inmunova, which is developing an immune biologic targeting Shiga toxin-producing *E. coli* infections, for which he receives no compensation, except for reimbursement of expenses. P.I.T. receives royalties from UpToDate from two sections on intestinal *E. coli* infections. G.D. is a consultant to and a member of the Scientific Advisory Board of Pluton Biosciences, which is developing methods for discovering environmental microbes for commercial applications. G.D. is a consultant to and a member of the Scientific Advisory Board of Claryx, which is developing methods for microbial surveillance in healthcare settings. G.D. has consulted for SNIPR Technologies Ltd. in the last 5 years but not presently.

STAR★METHODS

Detailed methods are provided in the online version of this paper and include the following:

- KEY RESOURCES TABLE
- METHOD DETAILS
  - Human gut microbiota associations
  - *In vivo* animal studies
  - Microbe strains
  - Pharmacokinetic experiments
  - Blood measurements
  - Gut permeability assays
  - RT-PCR
  - Metagenomic and genomic sequencing, analysis, and assembly
- QUANTIFICATION AND STATISTICAL ANALYSIS

SUPPLEMENTAL INFORMATION

Supplemental information can be found online at https://doi.org/10.1016/j.xcrm.2026.103161.

Received: March 16, 2026
Revised: September 28, 2026
Accepted: October 15, 2026

REFERENCES

1. Fleischmann, C., Reichert, F., Cassini, A., Horner, R., Harder, T., Markwart, R., Tröndle, M., Savova, Y., Kissoon, N., Schlattmann, P., et al. (2021). Global incidence and mortality of neonatal sepsis: a systematic review and meta-analysis. Arch. Dis. Child. *106*, 745–752. https://doi.org/10.1136/archdischild-2020-320217.
2. Dong, Y., and Speer, C.P. (2015). Late-onset neonatal sepsis: recent developments. Arch. Dis. Child. Fetal Neonatal Ed. *100*, F257–F263. https://doi.org/10.1136/archdischild-2014-306213.
3. Klinger, G., Reichman, B., Norman, M., Kusuda, S., Battin, M., Helenius, K., Isayama, T., Lui, K., Adams, M., Vento, M., et al. (2024). Late-Onset Sepsis among Extremely Preterm Infants of 24-28 Weeks Gestation: An International Comparison in 10 High-Income Countries. Neonatology *121*, 761–771. https://doi.org/10.1159/000539245.
4. Mukhopadhyay, S., Kaufman, D.A., Saha, S., Puopolo, K.M., Flannery, D.D., Weimer, K.E.D., Greenberg, R.G., Sanchez, P.J., Eichenwald, E.C., Cotten, C.M., et al. (2025). Late-Onset Sepsis Among Extremely Preterm Infants During the COVID-19 Pandemic. Pediatrics *155*, e2024067675. https://doi.org/10.1542/peds.2024-067675.
5. Rao, C., Coyte, K.Z., Bainter, W., Geha, R.S., Martin, C.R., and Rakoff-Nahoum, S. (2021). Multi-kingdom ecological drivers of microbiota assembly in preterm infants. Nature *591*, 633–638. https://doi.org/10.1038/s41586-021-03241-8.
6. Thänert, R., Schwartz, D.J., Keen, E.C., Hall-Moore, C., Wang, B., Shaikh, N., Ning, J., Rouggly-Nickless, L.C., Thänert, A., Ferreiro, A., et al. (2024). Clinical sequelae of gut microbiome development and disruption in hospitalized preterm infants. Cell Host Microbe *32*, 1822–1837.e5. https://doi.org/10.1016/j.chom.2024.07.027.
7. Schwartz, D.J., Shalon, N., Wardenburg, K., DeVeaux, A., Wallace, M.A., Hall-Moore, C., Ndao, I.M., Sullivan, J.E., Radmacher, P., Escobedo, M., et al. (2023). Gut pathogen colonization precedes bloodstream infection in the neonatal intensive care unit. Sci. Transl. Med. *15*, eadg5562. https://doi.org/10.1126/scitranslmed.adg5562.
8. Heston, S.M., Lim, C.S.E., Ong, C., Chua, M.C., Kelly, M.S., and Yeo, K.T. (2023). Strain-resolved metagenomic analysis of the gut as a reservoir for bloodstream infection pathogens among premature infants in Singapore. Gut Pathog. *15*, 55. https://doi.org/10.1186/s13099-023-00583-8.
9. Carl, M.A., Ndao, I.M., Springman, A.C., Manning, S.D., Johnson, J.R., Johnston, B.D., Burnham, C.-A.D., Weinstock, E.S., Weinstock, G.M., Wylie, T.N., et al. (2014). Sepsis From the Gut: The Enteric Habitat of Bacteria That Cause Late-Onset Neonatal Bloodstream Infections. Clin. Infect. Dis. *58*, 1211–1218. https://doi.org/10.1093/cid/ciu084.
10. Flannery, D.D., Ross, R.K., Mukhopadhyay, S., Tribble, A.C., Puopolo, K.M., and Gerber, J.S. (2018). Temporal Trends and Center Variation in Early Antibiotic Use Among Premature Infants. JAMA Netw. Open *1*, e180164. https://doi.org/10.1001/jamanetworkopen.2018.0164.
11. Gibson, M.K., Wang, B., Ahmadi, S., Burnham, C.-A.D., Tarr, P.I., Warner, B.B., and Dantas, G. (2016). Developmental dynamics of the preterm infant gut microbiota and antibiotic resistome. Nat. Microbiol. *1*, 16024. https://doi.org/10.1038/nmicrobiol.2016.24.
12. Tsai, M.H., Chu, S.M., Hsu, J.F., Lien, R., Huang, H.R., Chiang, M.C., Fu, R.H., Lee, C.W., and Huang, Y.C. (2015). Breakthrough bacteremia in the neonatal intensive care unit: incidence, risk factors, and attributable mortality. Am. J. Infect. Control *43*, 20–25. https://doi.org/10.1016/j.ajic.2014.09.022.
13. Singh, N., Patel, K.M., Léger, M.M., Short, B., Sprague, B.M., Kalu, N., and Campos, J.M. (2002). Risk of resistant infections with Enterobacteriaceae in hospitalized neonates. Pediatr. Infect. Dis. J. *21*, 1029–1033. https://doi.org/10.1097/00006454-200211000-00010.
14. Kuppala, V.S., Meinzen-Derr, J., Morrow, A.L., and Schibler, K.R. (2011). Prolonged initial empirical antibiotic treatment is associated with adverse outcomes in premature infants. J. Pediatr. *159*, 720–725. https://doi.org/10.1016/j.jpeds.2011.05.033.
15. Jiang, S., Yang, Z., Shan, R., Zhang, Y., Yan, W., Yang, Y., Shah, P.S., Lee, S.K., and Cao, Y.; Reduction of Infection in Neonatal Intensive Care Units using the Evidence-based Practice for Improving Quality Study Group (2020). Neonatal Outcomes Following Culture-negative Late-onset Sepsis Among Preterm Infants. Pediatr. Infect. Dis. J. *39*, 232–238. https://doi.org/10.1097/INF.0000000000002558.
16. Ting, J.Y., Synnes, A., Roberts, A., Deshpandey, A., Dow, K., Yoon, E.W., Lee, K.S., Dobson, S., Lee, S.K., and Shah, P.S.; Canadian Neonatal Network Investigators (2016). Association Between Antibiotic Use and Neonatal Mortality and Morbidities in Very Low-Birth-Weight Infants Without Culture-Proven Sepsis or Necrotizing Enterocolitis. JAMA

Please cite this article in press as: Schwartz et al., Microbiome-antibiotic-immune interactions influence mortality in preterm infant gut microbiota-humanized gnotobiotic mice, Cell Reports Medicine (2026), https://doi.org/10.1016/j.xcrm.2026.103161

Pediatr. *170*, 1181–1187. https://doi.org/10.1001/jamapediatrics.2016.2132.

17. Fajardo, C., Alshaikh, B., and Harabor, A. (2019). Prolonged use of antibiotics after birth is associated with increased morbidity in preterm infants with negative cultures. The journal of maternal-fetal & neonatal medicine : the official journal of the European Association of Perinatal Medicine, the Federation of Asia and Oceania Perinatal Societies. the International Society of Perinatal Obstet *32*, 4060–4066. https://doi.org/10.1080/14767058.2018.1481042.
18. Cantey, J.B., Pyle, A.K., Wozniak, P.S., Hynan, L.S., and Sánchez, P.J. (2018). Early Antibiotic Exposure and Adverse Outcomes in Preterm, Very Low Birth Weight Infants. J. Pediatr. *203*, 62–67. https://doi.org/10.1016/j.jpeds.2018.07.036.
19. Olin, A., Henckel, E., Chen, Y., Lakshmikanth, T., Pou, C., Mikes, J., Gustafsson, A., Bernhardsson, A.K., Zhang, C., Bohlin, K., and Brodin, P. (2018). Stereotypic Immune System Development in Newborn Children. Cell *174*, 1277–1292.e14. https://doi.org/10.1016/j.cell.2018.06.045.
20. Erickson, I., Tung, J., and Schwartz, D.J. (2025). Consequences of host-microbiome interactions in preterm infants. Infect. Immun. *93*, e0050124. https://doi.org/10.1128/iai.00501-24.
21. Park, S.Y., Lee, Y.Q., Kim, D., Sung, D.K., Kim, K.S., Lee, J.S., Cho, J.Y., Lee, W., Sung, S.I., and Lee, D.Y. (2025). Deciphering dynamic antibiotics-microbiome-metabolome interactions in preterm infants using systems biology. iScience *28*, 113038. https://doi.org/10.1016/j.isci.2025.113038.
22. Tu, V., Ren, Y., Tanes, C., Mukhopadhyay, S., Daniel, S.G., Li, H., and Bittinger, K. (2024). A quantitative approach to measure and predict microbiome response to antibiotics. mSphere *9*, e0048824. https://doi.org/10.1128/msphere.00488-24.
23. Prashant, A., Vishwanath, P., Kulkarni, P., Sathya Narayana, P., Gowdara, V., Nataraj, S.M., and Nagaraj, R. (2013). Comparative Assessment of Cytokines and Other Inflammatory Markers for the Early Diagnosis of Neonatal Sepsis–A Case Control Study. PLoS One *8*, e68426. https://doi.org/10.1371/journal.pone.0068426.
24. Cantey, J.B., and Lee, J.H. (2021). Biomarkers for the Diagnosis of Neonatal Sepsis. Clin. Perinatol. *48*, 215–227. https://doi.org/10.1016/j.clp.2021.03.012.
25. Russell, J.T., Lauren Ruoss, J., de la Cruz, D., Li, N., Bazacliu, C., Patton, L., McKinley, K.L., Garrett, T.J., Polin, R.A., Triplett, E.W., and Neu, J. (2021). Antibiotics and the developing intestinal microbiome, metabolome and inflammatory environment in a randomized trial of preterm infants. Sci. Rep. *11*, 1943. https://doi.org/10.1038/s41598-021-80982-6.
26. Singer, J.R., Blosser, E.G., Zindl, C.L., Silberger, D.J., Conlan, S., Laufer, V.A., DiToro, D., Deming, C., Kumar, R., Morrow, C.D., et al. (2019). Preventing dysbiosis of the neonatal mouse intestinal microbiome protects against late-onset sepsis. Nat. Med. *25*, 1772–1782. https://doi.org/10.1038/s41591-019-0640-y.
27. Deshmukh, H.S., Liu, Y., Menkiti, O.R., Mei, J., Dai, N., O'Leary, C.E., Oliver, P.M., Kolls, J.K., Weiser, J.N., and Worthen, G.S. (2014). The microbiota regulates neutrophil homeostasis and host resistance to Escherichia coli K1 sepsis in neonatal mice. Nat. Med. *20*, 524–530. https://doi.org/10.1038/nm.3542.
28. Schill, E.M., Joyce, E.L., Floyd, A.N., Udayan, S., Rusconi, B., Gaddipati, S., Barrios, B.E., John, V., Kaye, M.E., Kulkarni, D.H., et al. (2023). Vancomycin-induced gut microbial dysbiosis alters enteric neuron-macrophage interactions during a critical period of postnatal development. Front. Immunol. *14*, 1268909. https://doi.org/10.3389/fimmu.2023.1268909.
29. Knoop, K.A., McDonald, K.G., Kulkarni, D.H., and Newberry, R.D. (2016). Antibiotics promote inflammation through the translocation of native commensal colonic bacteria. Gut *65*, 1100–1109. https://doi.org/10.1136/gutjnl-2014-309059.
30. Kulkarni, D.H., McDonald, K.G., Knoop, K.A., Gustafsson, J.K., Kozlowski, K.M., Hunstad, D.A., Miller, M.J., and Newberry, R.D. (2018). Goblet cell associated antigen passages are inhibited during Salmonella typhimurium infection to prevent pathogen dissemination and limit responses to dietary antigens. Mucosal Immunol. *11*, 1103–1113. https://doi.org/10.1038/s41385-018-0007-6.
31. Zhang, L., Huang, Y., Zhou, Y., Buckley, T., and Wang, H.H. (2013). Antibiotic Administration Routes Significantly Influence the Levels of Antibiotic Resistance in Gut Microbiota. Antimicrob. Agents Chemother. *57*, 3659–3666. https://doi.org/10.1128/aac.00670-13.
32. Stewart, C.J., Ajami, N.J., O'Brien, J.L., Hutchinson, D.S., Smith, D.P., Wong, M.C., Ross, M.C., Lloyd, R.E., Doddapaneni, H., Metcalf, G.A., et al. (2018). Temporal development of the gut microbiome in early childhood from the TEDDY study. Nature *562*, 583–588. https://doi.org/10.1038/s41586-018-0617-x.
33. Sellers-Porter, C., Lueschow-Guijosa, S.R., Santana, J.M., Cera, A.J., Bautista, G.M., Persiani, M., Good, M., and McElroy, S.J. (2025). Modeling pathogen-driven neonatal late-onset sepsis: a modification to the murine cecal slurry. Front. Cell. Infect. Microbiol. *15*, 1589712. https://doi.org/10.3389/fcimb.2025.1589712.
34. Kannan, S.K., Kim, C.Y., Heidarian, M., Berton, R.R., Jensen, I.J., Griffith, T.S., and Badovinac, V.P. (2024). Mouse Models of Sepsis. Curr. Protoc. *4*, e997. https://doi.org/10.1002/cpz1.997.
35. Stark, A., Smith, P.B., Hornik, C.P., Zimmerman, K.O., Hornik, C.D., Pradeep, S., Clark, R.H., Benjamin, D.K., Jr., Laughon, M., and Greenberg, R.G. (2022). Medication Use in the Neonatal Intensive Care Unit and Changes from 2010 to 2018. J. Pediatr. *240*, 66–71.e4. https://doi.org/10.1016/j.jpeds.2021.08.075.
36. Ma, B., McComb, E., Gajer, P., Yang, H., Humphrys, M., Okogbule-Wonodi, A.C., Fasano, A., Ravel, J., and Viscardi, R.M. (2018). Microbial Biomarkers of Intestinal Barrier Maturation in Preterm Infants. Front. Microbiol. *9*, 2755. https://doi.org/10.3389/fmicb.2018.02755.
37. Warner, B.B., Deych, E., Zhou, Y., Hall-Moore, C., Weinstock, G.M., Sodergren, E., Shaikh, N., Hoffmann, J.A., Linneman, L.A., Hamvas, A., et al. (2016). Gut bacteria dysbiosis and necrotising enterocolitis in very low birthweight infants: a prospective case-control study. Lancet *387*, 1928–1936. https://doi.org/10.1016/s0140-6736(16)00081-7.
38. La Rosa, P.S., Warner, B.B., Zhou, Y., Weinstock, G.M., Sodergren, E., Hall-Moore, C.M., Stevens, H.J., Bennett, W.E., Jr., Shaikh, N., Linneman, L.A., et al. (2014). Patterned progression of bacterial populations in the premature infant gut. Proc. Natl. Acad. Sci. USA *111*, 12522–12527. https://doi.org/10.1073/pnas.1409497111.
39. Gasparrini, A.J., Wang, B., Sun, X., Kennedy, E.A., Hernandez-Leyva, A., Ndao, I.M., Tarr, P.I., Warner, B.B., and Dantas, G. (2019). Persistent metagenomic signatures of early-life hospitalization and antibiotic treatment in the infant gut microbiota and resistome. Nat. Microbiol. *4*, 2285–2297. https://doi.org/10.1038/s41564-019-0550-2.
40. Prusakov, P., Goff, D.A., Wozniak, P.S., Cassim, A., Scipion, C.E.A., Urzúa, S., Ronchi, A., Zeng, L., Ladipo-Ajayi, O., Aviles-Otero, N., et al. (2021). A global point prevalence survey of antimicrobial use in neonatal intensive care units: The no-more-antibiotics and resistance (NO-MAS-R) study. EClinicalMedicine *32*, 100727. https://doi.org/10.1016/j.eclinm.2021.100727.
41. Lutsar, I., Chazallon, C., Trafojer, U., de Cabre, V.M., Auriti, C., Bertaina, C., Calo Carducci, F.I., Canpolat, F.E., Esposito, S., Fournier, I., et al. (2020). Meropenem vs standard of care for treatment of neonatal late onset sepsis (NeoMero1): A randomised controlled trial. PLoS One *15*, e0229380. https://doi.org/10.1371/journal.pone.0229380.
42. Tremoulet, A., Le, J., Poindexter, B., Sullivan, J.E., Laughon, M., Delmore, P., Salgado, A., Ian-U Chong, S., Melloni, C., Gao, J., et al. (2014). Characterization of the population pharmacokinetics of ampicillin in neonates using an opportunistic study design. Antimicrob. Agents Chemother. *58*, 3013–3020. https://doi.org/10.1128/aac.02374-13.
43. Smith, P.B., Cohen-Wolkowiez, M., Castro, L.M., Poindexter, B., Bidegain, M., Weitkamp, J.-H., Schelonka, R.L., Ward, R.M., Wade, K., Valencia, G., et al. (2011). Population Pharmacokinetics of Meropenem in

Please cite this article in press as: Schwartz et al., Microbiome-antibiotic-immune interactions influence mortality in preterm infant gut microbiota-humanized gnotobiotic mice, Cell Reports Medicine (2026), https://doi.org/10.1016/j.xcrm.2026.103161

Plasma and Cerebrospinal Fluid of Infants With Suspected or Complicated Intra-abdominal Infections. Pediatr. Infect. Dis. J. *30*, 844–849. https://doi.org/10.1097/inf.0b013e31822e8b0b.

44. Germovsek, E., Lutsar, I., Kipper, K., Karlsson, M.O., Planche, T., Chazallon, C., Meyer, L., Trafojer, U.M.T., Metsvaht, T., Fournier, I., et al. (2018). Plasma and CSF pharmacokinetics of meropenem in neonates and young infants: results from the NeoMero studies. J. Antimicrob. Chemother. *73*, 1908–1916. https://doi.org/10.1093/jac/dky128.

45. Nicolau, D.P. (2008). Pharmacokinetic and pharmacodynamic properties of meropenem. Clin. Infect. Dis. *47*, S32–S40. https://doi.org/10.1086/590064.

46. Bax, R.P., Bastain, W., Featherstone, A., Wilkinson, D.M., Hutchison, M., and Haworth, S.J. (1989). The pharmacokinetics of meropenem in volunteers. J. Antimicrob. Chemother. *24*, 311–320. https://doi.org/10.1093/jac/24.suppl_a.311.

47. Nickols, W.A., Kuntz, T., Shen, J., Maharjan, S., Mallick, H., Franzosa, E.A., Thompson, K.N., Nearing, J.T., and Huttenhower, C. (2026). MaAsLin 3: refining and extending generalized multivariable linear models for meta-omic association discovery. Nat. Methods *23*, 554–564. https://doi.org/10.1038/s41592-025-02923-9.

48. CLSI (2016). Performance Standards for Antimicrobial Susceptibility Testing (Clinical and Laboratory Standards Institute).

49. Edwards, J.R. (1995). Meropenem: a microbiological overview. J. Antimicrob. Chemother. *36*, 1–17. https://doi.org/10.1093/jac/36.suppl_a.1.

50. Efremova, I., Maslennikov, R., Kudryavtseva, A., Avdeeva, A., Krasnov, G., Diatroptov, M., Bakhitov, V., Aliev, S., Sedova, N., Fedorova, M., et al. (2024). Gut Microbiota and Cytokine Profile in Cirrhosis. J. Clin. Transl. Hepatol. *12*, 689–700. https://doi.org/10.14218/JCTH.2024.00090.

51. Schirmer, M., Smeekens, S.P., Vlamakis, H., Jaeger, M., Oosting, M., Franzosa, E.A., Ter Horst, R., Jansen, T., Jacobs, L., Bonder, M.J., et al. (2016). Linking the Human Gut Microbiome to Inflammatory Cytokine Production Capacity. Cell *167*, 1125–1136.e8. https://doi.org/10.1016/j.cell.2016.10.020.

52. Chekeni, F.B., Elliott, M.R., Sandilos, J.K., Walk, S.F., Kinchen, J.M., Lazarowski, E.R., Armstrong, A.J., Penuela, S., Laird, D.W., Salvesen, G.S., et al. (2010). Pannexin 1 channels mediate 'find-me' signal release and membrane permeability during apoptosis. Nature *467*, 863–867. https://doi.org/10.1038/nature09413.

53. Silverman, W., Locovei, S., and Dahl, G. (2008). Probenecid, a gout remedy, inhibits pannexin 1 channels. Am. J. Physiol. Cell Physiol. *295*, C761–C767. https://doi.org/10.1152/ajpcell.00227.2008.

54. Makarenkova, H.P., and Shestopalov, V.I. (2014). The role of pannexin hemichannels in inflammation and regeneration. Front. Physiol. *5*, 63. https://doi.org/10.3389/fphys.2014.00063.

55. Chen, W., Zhu, S., Wang, Y., Li, J., Qiang, X., Zhao, X., Yang, H., D'Angelo, J., Becker, L., Wang, P., et al. (2019). Enhanced Macrophage Pannexin 1 Expression and Hemichannel Activation Exacerbates Lethal Experimental Sepsis. Sci. Rep. *9*, 160. https://doi.org/10.1038/s41598-018-37232-z.

56. Pelegrin, P., and Surprenant, A. (2006). Pannexin-1 mediates large pore formation and interleukin-1beta release by the ATP-gated P2X7 receptor. EMBO J. *25*, 5071–5082. https://doi.org/10.1038/sj.emboj.7601378.

57. Liu, B., Zheng, D., Zhou, S., Chen, L., and Yang, J. (2022). VFDB 2022: a general classification scheme for bacterial virulence factors. Nucleic Acids Res. *50*, D912–D917. https://doi.org/10.1093/nar/gkab1107.

58. Antypas, H., Schmidtchen, V., Staiger, W.I., Yanhong, L.I., Tan, R.J.W., Ng, K.K.F., Neo, C.J.Y., Radhesh, S.M., Tanoto, F.R., da Silva, R.A.G., et al. (2026). Loss of Fsr quorum sensing promotes biofilm formation and worsens outcomes in enterococcal infective endocarditis. Nat. Commun. *17*, 1668. https://doi.org/10.1038/s41467-026-68366-8.

59. Qin, X., Singh, K.V., Weinstock, G.M., and Murray, B.E. (2001). Characterization of fsr, a regulator controlling expression of gelatinase and serine protease in Enterococcus faecalis OG1RF. J. Bacteriol. *183*, 3372–3382. https://doi.org/10.1128/JB.183.11.3372-3382.2001.

60. Ye, Q., Du, L.Z., Shao, W.X., and Shang, S.Q. (2017). Utility of cytokines to predict neonatal sepsis. Pediatr. Res. *81*, 616–621. https://doi.org/10.1038/pr.2016.267.

61. Hibbert, J., Strunk, T., Simmer, K., Richmond, P., Burgner, D., and Currie, A. (2020). Plasma cytokine profiles in very preterm infants with late-onset sepsis. PLoS One *15*, e0232933. https://doi.org/10.1371/journal.pone.0232933.

62. Samara, J., Moossavi, S., Alshaikh, B., Ortega, V.A., Pettersen, V.K., Ferdous, T., Hoops, S.L., Soraisham, A., Vayalumkal, J., Dersch-Mills, D., et al. (2022). Supplementation with a probiotic mixture accelerates gut microbiome maturation and reduces intestinal inflammation in extremely preterm infants. Cell Host Microbe *30*, 696–711.e5. https://doi.org/10.1016/j.chom.2022.04.005.

63. Venkatesan, T., Rees, P., Gardiner, J., Battersby, C., Purkayastha, M., Gale, C., and Sutcliffe, A.G. (2023). National Trends in Preterm Infant Mortality in the United States by Race and Socioeconomic Status, 1995-2020. JAMA Pediatr. *177*, 1085–1095. https://doi.org/10.1001/jamapediatrics.2023.3487.

64. Zhang, J., Sun, X., Zhong, L., and Shen, B. (2021). IL-32 exacerbates adenoid hypertrophy via activating NLRP3-mediated cell pyroptosis, which promotes inflammation. Mol. Med. Rep. *23*, 226. https://doi.org/10.3892/mmr.2021.11865.

65. Shang, J., Xu, Y., Pu, S., Sun, X., and Gao, X. (2023). Role of IL-34 and its receptors in inflammatory diseases. Cytokine *171*, 156348. https://doi.org/10.1016/j.cyto.2023.156348.

66. Olm, M.R., Bhattacharya, N., Crits-Christoph, A., Firek, B.A., Baker, R., Song, Y.S., Morowitz, M.J., and Banfield, J.F. (2019). Necrotizing enterocolitis is preceded by increased gut bacterial replication, Klebsiella, and fimbriae-encoding bacteria. Sci. Adv. *5*, eaax5727. https://doi.org/10.1126/sciadv.aax5727.

67. Yue, J., Hua, M., Chen, N., Li, J., Liu, X., Duan, A., Wang, H., Du, P., Rong, C., Yang, D., and Chen, C. (2022). Role of the fsr Quorum-Sensing System in Enterococcus faecalis Bloodstream Infection. Appl. Environ. Microbiol. *88*, e0155122. https://doi.org/10.1128/aem.01551-22.

68. Mohamed, J.A., Huang, W., Nallapareddy, S.R., Teng, F., and Murray, B.E. (2004). Influence of origin of isolates, especially endocarditis isolates, and various genes on biofilm formation by Enterococcus faecalis. Infect. Immun. *72*, 3658–3663. https://doi.org/10.1128/iai.72.6.3658-3663.2004.

69. Thurlow, L.R., Thomas, V.C., Narayanan, S., Olson, S., Fleming, S.D., and Hancock, L.E. (2010). Gelatinase contributes to the pathogenesis of endocarditis caused by Enterococcus faecalis. Infect. Immun. *78*, 4936–4943. https://doi.org/10.1128/IAI.01118-09.

70. Flannery, D.D., Edwards, E.M., Puopolo, K.M., and Horbar, J.D. (2021). Early-Onset Sepsis Among Very Preterm Infants. Pediatrics *148*, e2021052456. https://doi.org/10.1542/peds.2021-052456.

71. Coggins, S.A., Zevallos Barboza, A., Puopolo, K.M., and Flannery, D.D. (2025). Late Antibiotic Use Among Preterm Infants Admitted to the Neonatal Intensive Care Unit. Pediatrics *156*, e2025071372. https://doi.org/10.1542/peds.2025-071372.

72. Jiang, S., Zhang, L., Yan, W., Li, S., Han, J., Zhou, Q., Yang, Y., Lee, S.K., and Cao, Y.; REIN-EPIQ Study Group (2021). Antibiotic Use in Neonatal Intensive Care Units in China: A Multicenter Cohort Study. J. Pediatr. *239*, 136–142.e4. https://doi.org/10.1016/j.jpeds.2021.08.067.

73. Cantey, J.B., and Patel, S.J. (2014). Antimicrobial Stewardship in the NICU. Infect. Dis. Clin. *28*, 247–261. https://doi.org/10.1016/j.idc.2014.01.005.

74. Leggett, R.M., Alcon-Giner, C., Heavens, D., Caim, S., Brook, T.C., Kujawska, M., Martin, S., Peel, N., Acford-Palmer, H., Hoyles, L., et al.

Please cite this article in press as: Schwartz et al., Microbiome-antibiotic-immune interactions influence mortality in preterm infant gut microbiota-humanized gnotobiotic mice, Cell Reports Medicine (2026), https://doi.org/10.1016/j.xcrm.2026.103161

(2020). Rapid MinION profiling of preterm microbiota and antimicrobial-resistant pathogens. Nat. Microbiol. *5*, 430–442. https://doi.org/10.1038/s41564-019-0626-z.

75. Turner, A.M., Kinsella, P., Miller, W.R., Carter, G.P., Tran, T.T., Howden, B.P., and Arias, C.A. (2025). Therapeutic approach to difficult-to-treat multidrug-resistant enterococcal infections. Antimicrob. Agents Chemother. *69*, e0106024. https://doi.org/10.1128/aac.01060-24.

76. Zeng, J., Teng, F., and Murray, B.E. (2005). Gelatinase is important for translocation of Enterococcus faecalis across polarized human enterocyte-like T84 cells. Infect. Immun. *73*, 1606–1612. https://doi.org/10.1128/IAI.73.3.1606-1612.2005.

77. Maharshak, N., Huh, E.Y., Paiboonrungruang, C., Shanahan, M., Thurlow, L., Herzog, J., Djukic, Z., Orlando, R., Pawlinski, R., Ellermann, M., et al. (2015). Enterococcus faecalis Gelatinase Mediates Intestinal Permeability via Protease-Activated Receptor 2. Infect. Immun. *83*, 2762–2770. https://doi.org/10.1128/IAI.00425-15.

78. Wray, G.M., Foster, S.J., Hinds, C.J., and Thiemermann, C. (2001). A cell wall component from pathogenic and non-pathogenic gram-positive bacteria (peptidoglycan) synergises with endotoxin to cause the release of tumour necrosis factor-alpha, nitric oxide production, shock, and multiple organ injury/dysfunction in the rat. Shock *15*, 135–142. https://doi.org/10.1097/00024382-200115020-00010.

79. Lubin, J.B., Green, J., Maddux, S., Denu, L., Duranova, T., Lanza, M., Wynosky-Dolfi, M., Flores, J.N., Grimes, L.P., Brodsky, I.E., et al. (2023). Arresting microbiome development limits immune system maturation and resistance to infection in mice. Cell Host Microbe *31*, 554–570.e7. https://doi.org/10.1016/j.chom.2023.03.006.

80. Knoop, K.A., Coughlin, P.E., Floyd, A.N., Ndao, I.M., Hall-Moore, C., Shaikh, N., Gasparrini, A.J., Rusconi, B., Escobedo, M., Good, M., et al. (2020). Maternal activation of the EGFR prevents translocation of gut-residing pathogenic Escherichia coli in a model of late-onset neonatal sepsis. Proc. Natl. Acad. Sci. USA *117*, 7941–7949. https://doi.org/10.1073/pnas.1912022117.

81. El Manouni El Hassani, S., Berkhout, D.J.C., Niemarkt, H.J., Mann, S., de Boode, W.P., Cossey, V., Hulzebos, C.V., van Kaam, A.H., Kramer, B.W., van Lingen, R.A., et al. (2019). Risk Factors for Late-Onset Sepsis in Preterm Infants: A Multicenter Case-Control Study. Neonatology *116*, 42–51. https://doi.org/10.1159/000497781.

82. Soto Ocaña, J., Friedman, E.S., Keenan, O., Bayard, N.U., Ford, E., Tanes, C., Munneke, M.J., Beavers, W.N., Skaar, E.P., Bittinger, K., et al. (2024). Metal availability shapes early life microbial ecology and community succession. mBio *15*, e0153424. https://doi.org/10.1128/mbio.01534-24.

83. Bogaert, D., van Beveren, G.J., de Koff, E.M., Lusarreta Parga, P., Balcazar Lopez, C.E., Koppensteiner, L., Clerc, M., Hasrat, R., Arp, K., Chu, M.L.J.N., et al. (2023). Mother-to-infant microbiota transmission and infant microbiota development across multiple body sites. Cell Host Microbe *31*, 447–460.e6. https://doi.org/10.1016/j.chom.2023.01.018.

84. Conrey, P.E., Denu, L., O'Boyle, K.C., Rozich, I., Green, J., Maslanka, J., Lubin, J.B., Duranova, T., Haltzman, B.L., Gianchetti, L., et al. (2023). IgA deficiency destabilizes homeostasis toward intestinal microbes and increases systemic immune dysregulation. Sci. Immunol. *8*, eade2335. https://doi.org/10.1126/sciimmunol.ade2335.

85. Beck, L.C., Masi, A.C., Young, G.R., Vatanen, T., Lamb, C.A., Smith, R., Coxhead, J., Butler, A., Marsland, B.J., Embleton, N.D., et al. (2022). Strain-specific impacts of probiotics are a significant driver of gut microbiome development in very preterm infants. Nat. Microbiol. *7*, 1525–1535. https://doi.org/10.1038/s41564-022-01213-w.

86. Kiu, R., Darby, E.M., Alcon-Giner, C., Acuna-Gonzalez, A., Camargo, A., Lamberte, L.E., Phillips, S., Sim, K., Shaw, A.G., Clarke, P., et al. (2025). Impact of early life antibiotic and probiotic treatment on gut microbiome and resistome of very-low-birth-weight preterm infants. Nat. Commun. *16*, 7569. https://doi.org/10.1038/s41467-025-62584-2.

87. Kulkarni, T., Majarikar, S., Deshmukh, M., Ananthan, A., Balasubramanian, H., Keil, A., and Patole, S. (2022). Probiotic sepsis in preterm neonates-a systematic review. Eur. J. Pediatr. *181*, 2249–2262. https://doi.org/10.1007/s00431-022-04452-5.

88. Alshaikh, B.N., Ting, J., Lee, S., Lemyre, B., Wong, J., Afifi, J., Beltempo, M., and Shah, P.S.; Canadian Neonatal Network Investigators (2025). Effectiveness and Risks of Probiotics in Preterm Infants. Pediatrics *155*, e2024069102. https://doi.org/10.1542/peds.2024-069102.

89. Waschina, S., Pagel, J., Seeger, K., Pasderski, E., Rühlemann, M., Froitzheim, S., Künzel, S., Sommer, F., Franzenburg, S., Fortmann, I., et al. (2025). Bacterial metabolite patterns of infants receiving multi-strain probiotics and risk of late-onset sepsis. Cell Rep. *44*, 116431. https://doi.org/10.1016/j.celrep.2025.116431.

90. Shenoy, M.K., Rico, D.M., Lorant, A.K., Touré, H., Gordon, S., Milburn, L.J., Schwensen, J.S., Cabán, M.E., and Koch, M.A. (2025). Breast milk IgG engages the mouse neonatal immune system to instruct responses to gut antigens. Science (New York, N.Y.) *389*, eado5294. https://doi.org/10.1126/science.ado5294.

91. Maier, L., Goemans, C.V., Wirbel, J., Kuhn, M., Eberl, C., Pruteanu, M., Müller, P., Garcia-Santamarina, S., Cacace, E., Zhang, B., et al. (2021). Unravelling the collateral damage of antibiotics on gut bacteria. Nature *599*, 120–124. https://doi.org/10.1038/s41586-021-03986-2.

92. Lemme-Dumit, J.M., Song, Y., Lwin, H.W., Hernandez-Chavez, C., Sundararajan, S., Viscardi, R.M., Ravel, J., Pasetti, M.F., and Ma, B. (2022). Altered Gut Microbiome and Fecal Immune Phenotype in Early Preterm Infants With Leaky Gut. Front. Immunol. *13*, 815046. https://doi.org/10.3389/fimmu.2022.815046.

93. Murray, B.E., Singh, K.V., Ross, R.P., Heath, J.D., Dunny, G.M., and Weinstock, G.M. (1993). Generation of restriction map of Enterococcus faecalis OG1 and investigation of growth requirements and regions encoding biosynthetic function. Journal of Bacteriology *175*, 5216–5223. https://doi.org/10.1128/jb.175.16.5216-5223.1993.

94. Sifri, C.D., Mylonakis, E., Singh, K.V., Qin, X., Garsin, D.A., Murray, B.E., Ausubel, F.M., and Calderwood, S.B. (2002). Virulence effect of Enterococcus faecalis protease genes and the quorum-sensing locus fsr in Caenorhabditis elegans and mice. Infect. Immun. *70*, 5647–5650. https://doi.org/10.1128/IAI.70.10.5647-5650.2002.

95. Beghini, F., McIver, L.J., Blanco-Míguez, A., Dubois, L., Asnicar, F., Maharjan, S., Mailyan, A., Manghi, P., Scholz, M., Thomas, A.M., et al. (2021). Integrating taxonomic, functional, and strain-level profiling of diverse microbial communities with bioBakery 3. eLife *10*, e65088. https://doi.org/10.7554/eLife.65088.

96. Bolger, A.M., Lohse, M., and Usadel, B. (2014). Trimmomatic: a flexible trimmer for Illumina sequence data. Bioinformatics *30*, 2114–2120. https://doi.org/10.1093/bioinformatics/btu170.

97. Schmieder, R., and Edwards, R. (2011). Fast identification and removal of sequence contamination from genomic and metagenomic datasets. PLoS One *6*, e17288. https://doi.org/10.1371/journal.pone.0017288.

98. Bushnell, B. (2014). BBMap: Short read-aligner. https://sourceforge.net/projects/bbmap/.

99. Kaminski, J., Gibson, M.K., Franzosa, E.A., Segata, N., Dantas, G., and Huttenhower, C. (2015). High-Specificity Targeted Functional Profiling in Microbial Communities with ShortBRED. PLoS Comput. Biol. *11*, e1004557. https://doi.org/10.1371/journal.pcbi.1004557.

100. Gurevich, A., Saveliev, V., Vyahhi, N., and Tesler, G. (2013). QUAST: quality assessment tool for genome assemblies. Bioinformatics *29*, 1072–1075. https://doi.org/10.1093/bioinformatics/btt086.

101. Parks, D.H., Imelfort, M., Skennerton, C.T., Hugenholtz, P., and Tyson, G.W. (2015). CheckM: assessing the quality of microbial genomes recovered from isolates, single cells, and metagenomes. Genome Res. *25*, 1043–1055. https://doi.org/10.1101/gr.186072.114.

102. Brown, J., Pirrung, M., and McCue, L.A. (2017). FQC Dashboard: integrates FastQC results into a web-based, interactive, and extensible

Please cite this article in press as: Schwartz et al., Microbiome-antibiotic-immune interactions influence mortality in preterm infant gut microbiota-humanized gnotobiotic mice, Cell Reports Medicine (2026), https://doi.org/10.1016/j.xcrm.2026.103161

FASTQ quality control tool. Bioinformatics *33*, 3137–3139. https://doi.org/10.1093/bioinformatics/btx373.

103. Bankevich, A., Nurk, S., Antipov, D., Gurevich, A.A., Dvorkin, M., Kulikov, A.S., Lesin, V.M., Nikolenko, S.I., Pham, S., Prjibelski, A.D., et al. (2012). SPAdes: a new genome assembly algorithm and its applications to single-cell sequencing. J. Comput. Biol. *19*, 455–477. https://doi.org/10.1089/cmb.2012.0021.

104. Nurk, S., Meleshko, D., Korobeynikov, A., and Pevzner, P.A. (2017). metaSPAdes: a new versatile metagenomic assembler. Genome Res. *27*, 824–834. https://doi.org/10.1101/gr.213959.116.

105. Li, H. (2013). Aligning sequence reads, clone sequences and assembly contigs with BWA-MEM, arXiv:1303.3997v2. https://doi.org/10.48550/arXiv.1303.3997.

106. Danecek, P., Bonfield, J.K., Liddle, J., Marshall, J., Ohan, V., Pollard, M.O., Whitwham, A., Keane, T., McCarthy, S.A., Davies, R.M., and Li, H. (2021). Twelve years of SAMtools and BCFtools. GigaScience *10*, giab008. https://doi.org/10.1093/gigascience/giab008.

107. Kang, D.D., Li, F., Kirton, E., Thomas, A., Egan, R., An, H., and Wang, Z. (2019). MetaBAT 2: an adaptive binning algorithm for robust and efficient genome reconstruction from metagenome assemblies. PeerJ *7*, e7359. https://doi.org/10.7717/peerj.7359.

108. Chaumeil, P.A., Mussig, A.J., Hugenholtz, P., and Parks, D.H. (2022). GTDB-Tk v2: memory friendly classification with the genome taxonomy database. Bioinformatics *38*, 5315–5316. https://doi.org/10.1093/bioinformatics/btac672.

109. Waters, C.M., Antiporta, M.H., Murray, B.E., and Dunny, G.M. (2003). Role of the Enterococcus faecalis GelE protease in determination of cellular chain length, supernatant pheromone levels, and degradation of fibrin and misfolded surface proteins. J. Bacteriol. *185*, 3613–3623. https://doi.org/10.1128/JB.185.12.3613-3623.2003.

110. Wexler, P., and Anderson, B.D. (2014). Encyclopedia of Toxicology, Third edition (Academic Press is an imprint of Elsevier).

111. Onyeji, C.O., Bui, K.Q., Nicolau, D.P., Nightingale, C.H., Bow, L., and Quintiliani, R. (1999). Influence of adjunctive interferon-gamma on treatment of gentamicin- and vancomycin-resistant Enterococcus faecalis infection in mice. Int. J. Antimicrob. Agents *12*, 301–309. https://doi.org/10.1016/s0924-8579(99)00055-2.

112. Hawk, C.T., Leary, S.L., and Morris, T.H.American College of Laboratory Animal Medicine; European College of Laboratory Animal Medicine (2005). Formulary for Laboratory Animals, 3rd Edition (Blackwell Pub.).

113. Schwartz, D.J., Conover, M.S., Hannan, T.J., and Hultgren, S.J. (2015). Uropathogenic Escherichia coli Superinfection Enhances the Severity of Mouse Bladder Infection. PLoS Pathog. *11*, e1004599. https://doi.org/10.1371/journal.ppat.1004599.

114. Wang, L., Llorente, C., Hartmann, P., Yang, A.M., Chen, P., and Schnabl, B. (2015). Methods to determine intestinal permeability and bacterial translocation during liver disease. J. Immunol. Methods *421*, 44–53. https://doi.org/10.1016/j.jim.2014.12.015.

115. Alcock, B.P., Raphenya, A.R., Lau, T.T.Y., Tsang, K.K., Bouchard, M., Edalatmand, A., Huynh, W., Nguyen, A.L.V., Cheng, A.A., Liu, S., et al. (2019). CARD 2020: antibiotic resistome surveillance with the comprehensive antibiotic resistance database. Nucleic Acids Res. *48*, D517–D525. https://doi.org/10.1093/nar/gkz935.

Please cite this article in press as: Schwartz et al., Microbiome-antibiotic-immune interactions influence mortality in preterm infant gut microbiota-humanized gnotobiotic mice, Cell Reports Medicine (2026), https://doi.org/10.1016/j.xcrm.2026.103161

STAR★METHODS

KEY RESOURCES TABLE

REAGENT or RESOURCE	SOURCE	IDENTIFIER
Bacterial and virus strains		
Human preterm infant gut microbiome samples	this paper, Gibson et al.,[11] Gasparrini et al.,[39] Schwartz et al.,[7] Warner et al.,[37] La Rosa et al.,[38] Thänert et al.[6]	Neonatal Microbiome and Necrotizing Enterocolitis cohort
Enterococcus faecalis from preterm infant stool	this paper	Neonatal Microbiome and Necrotizing Enterocolitis cohort
OG1RF	Murray et al.[93]	OG1RF
TX5264 (OG1RF Δ*gelE*)	Sifri et al.[94]	TX5264 (OG1RF Δ*gelE*)
TX5266 (OG1RF Δ*fsrB*)	Sifri et al.[94]	TX5266 (OG1RF Δ*fsrB*)
Biological samples		
Human preterm infant gut microbiome samples	this paper, Gibson et al.,[11] Gasparrini et al.,[39] Schwartz et al.,[7] Warner et al.,[37] La Rosa et al.,[38] Thänert et al.[6]	Neonatal Microbiome and Necrotizing Enterocolitis cohort
Human preterm infant remnant blood samples	this paper, Gibson et al.,[11] Gasparrini et al.,[39] Schwartz et al.,[7] Warner et al.,[37] La Rosa et al.,[38] Thänert et al.[6]	Neonatal Microbiome and Necrotizing Enterocolitis cohort
Chemicals, peptides, and recombinant proteins		
Antibiotics	Sigma	A9393, M2574, V2002, G3632
Probenecid	ThermoFisher	P36400
40 kDa FITC-dextran	Sigma	FD40
Critical commercial assays		
Bio-plex Pro Mouse Cytokine 23-plex Assay	BIO-Rad	M60009RDPD
Bio-Plex Pro Human Inflammation Panel 1	BIO-Rad	171AL001M
DNeasy/MagAttract Powersoil Pro Kit	Qiagen	Cat #47014, cat #47119
Nextera XT kit	Illumina	Cat #20034197
RT-PCR for panx1	ThermoFisher	Assay ID: Mm00450900_m1, Cat# 4351370; Assay ID: Mm99999915_g1, Cat.# 4331182
Biostic Bacteremia Kit	Qiagen	Cat #12240
Deposited data		
Metagenomic and genomic DNA, genomic and MAG assemblies	this paper	NCBI: BioProject PRJNA1402348
Metagenomic DNA	Gibson et al.[11]	NCBI: BioProject PRJNA301903
Metagenomic DNA	Gasparrini et al.[39]	NCBI: BioProject PRJNA489090
Metagenomic DNA	Schwartz et al.[7]	NCBI: BioProject PRJNA884103
Metagenomic DNA	Thänert et al.[6]	NCBI: BioProject PRJNA799247
Experimental models: Organisms/strains		
Mouse: C57BL6, WT conventional and WT germ-free	Jackson	C57BL6/J
Oligonucleotides		
gelE: TTGTCCGTGTTTACTTGGCG-AGGACAATCAGGTGCCTTGA	Sifri et al.[94]	gelE
fsrB: TCTAGGCTTAGTTCCCACACC-GTCTCGTCATCCAAGGTCT	Sifri et al.[94]	fsrB
Software and algorithms		
AB Sciex Analyst v1.6.3	Sciex	https://sciex.com/ec/products/software/analyst-software
MetaPhlAn3 v3.1	Beghini et al.[95]	https://github.com/biobakery/metaphlan

(*Continued on next page*)

Please cite this article in press as: Schwartz et al., Microbiome-antibiotic-immune interactions influence mortality in preterm infant gut microbiota-humanized gnotobiotic mice, Cell Reports Medicine (2026), https://doi.org/10.1016/j.xcrm.2026.103161

CellPress
OPEN ACCESS

Continued

REAGENT or RESOURCE	SOURCE	IDENTIFIER
MaAsLin3	Nickols et al.[47]	https://github.com/biobakery/maaslin3
Trimmomatic@0.39	Bolger et al.[96]	https://github.com/usadellab/trimmomatic
Deconseq v0.4.3	Schmieder et al.[97]	https://deconseq.sourceforge.net/
BBmap@39.01	Bushnell et al.[98]	https://sourceforge.net/projects/bbmap/
ShortBRED quantify v0.9.4	Kaminski et al.[99]	https://github.com/biobakery/shortbred
Quast v3.2	Gurevich et al.[100]	https://github.com/ablab/quast
CheckM v1.0.13-python-2.7.15	Parks et al.[101]	https://github.com/ecogenomics/checkm
FastQC	Brown et al.[102]	https://github.com/s-andrews/fastqc
SPAdes v3.1.0	Bankevich et al.[103]	https://github.com/ablab/spades
MetaSPAdes v4.2.0	Nurk et al.[104]	https://github.com/ablab/spades
BWA-MEM v0.7.17	Li et al.[105]	https://github.com/lh3/BWA
SAMtools v1.19.2	Danecek et al.[106]	https://github.com/samtools
MetaBAT2 v2.15	Kang et al.[107]	https://github.com/taffish/metabat2
GTDB-Tk (v2.3.2)	Chaumeil et al.[108]	https://github.com/ecogenomics/gtdbtk
GraphPad Prism v10	Graphpad Prism	https://Graphpad.com
Rstudio V2024.09.1-V2026.05.1	Rstudio	posit.co
R v4.4.2–4.6.0	R core team	https://www.r-project.org
Custom code and analysis scripts	this paper	https://github.com/DJSchwartzLab/NICUmousemodel https://doi.org/10.5281/zenodo.23070073

METHOD DETAILS

Human gut microbiota associations

3089 previously published metagenomes (BioProjects PRJNA301903, PRJNA489090, PRJNA884103, PRJNA799247) from 266 hospitalized preterm infants[6,7,11,39] were processed with MetaPhlAn3[95] at the species level (Data S2). Meropenem exposure in the prior 1, 3, and 7 days was determined relative to the day of fecal sample collection (Data S1). Associations between species-level taxonomic composition and meropenem exposure, DOL, gestational age, fraction of days without feeding (NPO), fraction of days of human milk, fraction of days of formula, delivery mode, and final disposition were determined with MaAsLin3[47] using default parameters and included a minimum prevalence filter (–min_prevalence) of 1%. Subject was included as a random effect. Sex was not included as a variable in these analyses. For display, the top 10 associations are plotted on the heatmap with full significant results ($q < 0.1$ per default) available in Data S4. Secondary analysis was approved under Washington University School of Medicine HRPO #201205152.

In vivo animal studies

The IACUC of Washington University School of Medicine approved all animal experiments. WT conventional C57BL6/J mice were sourced from Jackson labs and maintained under specific pathogen free conditions. A colony of germ-free mice originally sourced from Jackson labs has been maintained at Washington University School of Medicine for gnotobiotic experiments and rederived every 3–4 years. Confirmation of germ-free status in the colony was performed at least monthly with aerobic and anaerobic cultures and 16S rRNA gene amplification. A fecal sample prior to microbiota gavage was shotgun sequenced to confirm absence of microbes. Mice were maintained on a strict 12-h light/dark cycle except for a 45-min period each evening for one antibiotic administration at midnight. They were fed autoclaved mouse chow (LabDiet: Standard Diet 5021 - Autoclavable Mouse Breeder). Breeding pairs consisting of 1 male and 1 female in each cage were set up in sterile flexible vinyl isolators. At the time of mating, 200–300 μL of a clarified fecal sample was orally gavaged into dams after gentle restraint for microbiota-humanization experiments. Inocula were plated on MacConkey and Enterococcosel agar. Mouse pups were cross-fostered between litters of the same microbiota if their birth occurred within 5 days and allowed to acclimatize at least 2 days prior to manipulation. Gnotobiotic mouse experiments were conducted in flexible isolators with up to 3 cages in each isolator. A subset of experiments was conducted in the Washington University Gnotobiotic Core Facility in Allentown racks with 1 male in a cage with 2 female mice. Prior to each manipulation, cages were sterilized in the pass-through chamber with Clidox for 20 min followed by manipulation in a biosafety cabinet. Fresh fecal samples were obtained by combined application of gentle suprapubic and posterior dorsal pressure into a sterile, pre-weighed Eppendorf tube. Blood of live animals was obtained by cheek poke with a 5mm lancet and placed in EDTA tubes. Mice were weighed daily during antibiotic treatment to adjust antibiotic concentrations and monitor health. Subcutaneous antibiotic injections every 8 h were administered to pups of both sexes for 3 days between average postnatal day 10–12 with pup sacrifice on postnatal day 13 or 14. Antibiotics were administered at a sliding scale volume to ensure mg/kg body weight dosing as determined through pharmacokinetic

Please cite this article in press as: Schwartz et al., Microbiome-antibiotic-immune interactions influence mortality in preterm infant gut microbiota-humanized gnotobiotic mice, Cell Reports Medicine (2026), https://doi.org/10.1016/j.xcrm.2026.103161

experiments outlined below. Mouse pups that lost greater than 20% of starting body weight were euthanized and included in data analysis. Animals found deceased and intact were promptly removed, sprayed with 70% ethanol and organs were extracted for plating of spleens, livers, and colon washes. Spleen, liver, and colon washes in 1 mL PBS were plated on MacConkey agar with and without ampicillin, brain heart infusion (BHI) agar, and/or Enterococcosel agar (BD). Fecal samples were weighed and resuspended in 100 μL and serially diluted and plated on the agars listed above. When no colonies were detected on plating, values were set to the limit of detection (LOD) of 1 CFU based on the weight of the fecal sample. Despite every 8-h welfare checks, some animals were found deceased and eaten. These animals were included in survival and microbiota analyses from prior samples, but no postmortem microbiota sequencing or culturing was performed. Surviving animals not meeting humane endpoint criteria of weight loss were anesthetized with 4% isofluorane and cardiac blood was extracted for cytokine analysis. Animals were then sacrificed with isofluorane anesthesia and cervical dislocation, and organs were harvested. Sex was recorded where possible, but was not included as a variable in survival or microbiota analysis.

Microbe strains

Bulk fecal samples for inoculation into germ-free mice were derived from a previously completed study to determine the role of the preterm gut microbiota on necrotizing enterocolitis.[6,7,11,37–39] Selected samples were chosen based on prior shotgun metagenomic sequencing efforts to reflect key early-life microbiota compositions.[11,39] A portion was plated on LB and BHI agar to confirm viability prior to selection. Portions of fecal samples frozen at −80°C were chipped on dry ice into sterile tubes and resuspended 1:20 weight:-volume to a final concentration of 15% glycerol in PBS with 0.5% cysteine into cryovials. 10 μL from each inoculum was plated to enumerate CFUs and shotgun metagenomically sequenced.

Enterococcus faecalis was obtained from microbiota by plating to Enterococcosel agar. Single colonies were picked and underwent whole genome sequencing. MIC testing to ampicillin, meropenem, and imipenem was performed using an Etest (meropenem) or Kirby-Bauer disk diffusion (ampicillin/imipenem) using CLSI breakpoints, where applicable.[48] MALDI from bacterial isolates from dead animals was performed on the VITEK MALDI-TOF MS v2.3.3 (bioMérieux) per manufacturer instructions. Single colonies were used directly from MacConkey plates.

Gelatinase activity of *Enterococcus faecalis* strains was assessed using methods adapted from Waters et al. 2003.[109] Isolates were cultured overnight in BHI broth, then diluted with sterile PBS to an OD_{600} of 0.5. 2 μL of each diluted culture was spotted on BHI agar supplemented with 3% gelatin (AZER-ES17536), then cultured overnight at 37°C. Plates were transferred to 4°C. After four hours, gelatinase-positive cultures exhibited a white halo. OG1RF was used as a positive control for gelatinase activity (Gel+) and TX5264 (OG1RF Δ*gelE*) was used as a negative control.

The *gelE* and *fsr* genotypes of each strain were confirmed with PCR. 25 μl PCR reactions were created using Thermo Scientific 2× PCR Master Mix (K0171) and contained: 0.05 U/μL *Taq* DNA polymerase, 4 mM $MgCl_2$, 0.4 mM dATP, 0.4 mM dATP, 0.4 mM dTTP, 0.4 mM dCTP, 0.4 mM dGTP, reaction buffer, 0.5 pg to 0.5 ng DNA template, and 0.4 μM forward and reverse primers (gelE: TTGTCCGTGTTTACTTGGCG- AGGACAATCAGGTGCCTTGA; fsrB: TCTAGGCTTAGTTCCCACACC-GTCTCGTCATCCAAGGTCT). Reaction conditions were as follows: denaturation at 95°C for 2 min, then 30 cycles of 95°C for 30 s, 60°C for 30 s, and 72°C for 25 s, followed by 10 min at 72°C. OG1RF was used as a positive control for *gelE* and *fsrB*, while TX5264 (OG1RF Δ*gelE*) and TX5266 (OG1RF Δ*fsrB*) were used as negative controls.[59,94]

Pharmacokinetic experiments

Conventional wild-type C57BL/6 mice between p8 and p16 were subcutaneously injected with ampicillin, vancomycin, or meropenem with or without probenecid (ThermoFisher P36400) in 50–200 μL PBS for serum pharmacokinetic determination. Mice were anesthetized under 4% isofluorane, and cardiac puncture was performed to obtain terminal blood. Blood was centrifuged 10,000 × g for 10 min at 4C in serum separator tubes (BD). Serum antibiotic concentrations were measured using liquid chromatography-mass spectrometry with the following protocol. All standards and samples were kept on ice during preparation. Ampicillin and meropenem standards were prepared at 1 mg/mL in DMSO. D_6-meropenem and D_5-ampicillin internal standards were also prepared at 1 mg/mL in DMSO. These were dissolved in HPLC-grade acetonitrile to a final concentration of 3 μg/mL. Standard curves for meropenem and ampicillin were constructed by serial dilution of the 1 mg/mL stocks in DMSO, starting at 333 μg/mL. To control for matrix effects, 2.5 μL of each standard was mixed thoroughly with 22.5 μL of untreated murine serum. Samples were diluted in 100 μL of the internal standard mix and immediately vortexed. Precipitates were removed by centrifuging at 14,000 rpm at 4°C for 10 min. To match the DMSO content of the standard curve, 2.5 μL of DMSO was added to 22.5 μL of sera from antibiotic-treated mice and thoroughly mixed. Sera were then precipitated with internal standard mix and spun down in the same way as the standard samples. Samples were injected (2 μL) using a Shimadzu UHPLC and separated on an Ascentis-Express fused core phenyl-hexyl column (100 mm × 2 mm x 2.7 μm) using a flow rate of 0.4 mL/min. Proportions of mobile phase solvents A (0.1% formic acid in H2O) and B (90% acetonitrile, 0.1% formic acid in H2O) were varied. Antibiotics and internal standards were detected with an AB Sciex 4000 QTrap triple-quadrupole mass spectrometer. Samples were analyzed in positive-ion modes using a Turbo V electrospray ionization source with ion spray voltage set to 3000 V and heater temperature at 500°C. Ion source gas 1 and 2 were set to 40 and 35, respectively, and curtain gas set to 10. Collision gas flow was set to "medium". Each analyte was monitored using the precursor/product-ion pairs (meropenem 384.3/141.1 m/z, D_6-meropenem 390.3/147.1, ampicillin 350.3/160.1 m/z, D_5-ampicillin

Please cite this article in press as: Schwartz et al., Microbiome-antibiotic-immune interactions influence mortality in preterm infant gut microbiota-humanized gnotobiotic mice, Cell Reports Medicine (2026), https://doi.org/10.1016/j.xcrm.2026.103161

355.3/196.9 m/z). For all metabolites, EP was set to 10 V. Peak areas were integrated using AB Sciex Analyst software version 1.6.3 and normalized by dividing each antibiotic peak area by its corresponding internal standard peak area.

Antibiotic doses for subsequent gnotobiotic experiments were determined empirically from these pharmacokinetic experiments. We assumed first-order kinetics for β-lactams and calculated the elimination rate constant (k_{el} = −2.303*slope) of the linear regression of $\log_{10}$ concentration versus time curve.[45,110] We determined half-life as 0.693/k_{el} and time above minimum inhibitory concentration ($T_{>MIC}$) as the number of half-lives above maximum concentration divided by MIC. Gentamicin dosing was adapted from prior literature stating that 12–40 mg/kg once daily provided killing of *E. faecalis* without overt toxicity.[111,112]

Blood measurements

Mouse Cardiac blood was centrifuged at 4°C in Vacutainer serum separator tubes (BD) for 10 min at 10,000 × g prior to freezing at −80°C until use. Available remnant plasma from infants in our study within 10 days before and 7 days after meropenem was used to evaluate cytokine differences. BioRad BioPlex cytokine arrays were used as per manufacturer's instructions except the kit was used at half concentration.[113] Observations below the limit of quantitation were set to the lower limit of quantitation.

Gut permeability assays

To evaluate gut permeability after antibiotic administration, 40 kDa FITC-dextran (Sigma) was dissolved in PBS and 100 μL of 40 mg/mL (target 600 mg/kg/mouse[114]) was orally gavaged two hours after subcutaneous antibiotic administration. Four hours later, blood was obtained as above and FITC was measured at 530 nm after excitement at 490nm. Values were obtained with reference to a standard curve at 10-fold dilutions.

RT-PCR

Total RNA was isolated from colons using the Trizol reagent kit per the manufacturer's instructions and reversely transcribed into the first-strand cDNA using the SuperScript IV VILO with ezDNase (ThermoFisher). Following reverse transcription, a panel of established primers and probe for murine panx1 (Assay ID: Mm00450900_m1, Cat# 4351370, ThermoFisher Scientific), and glyceraldehyde 3-phosphate dehydrogenase gene (Assay ID: Mm99999915_g1, Cat.# 4331182, ThermoFisher Scientific) were used to quantify the Panx1 mRNA expression values using a QuantStudio 3 system. Amplification was performed using the Taqman Universal Master Mix II with UNG Mastermix under the following conditions: 95°C 10′; followed by 40 cycles of 95°C for 15″ and 60°C for 1′. The relative fold *panx1* mRNA expression[55] was calculated using the following formula: $\Delta\Delta = 2^{-\Delta\Delta Ct}$, where ΔΔCt = ΔCt (treated group) −ΔCt (PBS group), ΔCt = Ct (panx1) − Ct (GAPDH), and Ct = cycle at which the threshold was reached. Each sample was run in duplicate with and without the addition of reverse transcriptase.

Metagenomic and genomic sequencing, analysis, and assembly

Fecal samples or colon washes were extracted using the Qiagen Powersoil Pro kit or the MagAttract Powersoil Pro kit on the KingFisher Apex. Genomic DNA from bacterial isolates after overnight incubation was extracted with the Biostic Bacteremia kit. Nextera library preparation and sequencing were performed on the NextSeq 6000 or NovaSeq X. Sequencing adapters were trimmed with trimmomatic@0.39,[96] sequencing reads matching the mouse or human chromosome were removed with Deconseq v.0.4.3,[97] reads were repaired with BBmap@39.01.[98] Taxonomy was assigned with MetaPhlAn v3.1.0.[95] ShortBRED quantify v0.9.4 with reference to the 2020 CARD database and NCBI AMR catalog was used with 95% identity[99,115] to assign antibiotic resistance genes to metagenomes. Bacterial genome assemblies were created with SPAdes[103] and quality control was performed with Quast v3.2[100] and CheckM v1.0.13-python-2.7.15.[101] MAGs from previously sequenced human samples during NICU hospitalization[6,7,11,39] were assembled with the following protocol. Read quality was assessed using FastQC (v0.12.1).[102] If adapter contamination was detected, reads were trimmed using Trimmomatic (v0.39) with the appropriate adapter file (TruSeq3-PE-2.fa or NexteraPE-PE.fa).[96] Metagenomic reads were re-paired and filtered using the repair.sh script in BBMap (v39.01) with the –tossbrokenreads flag.[98] Each metagenome was assembled independently using MetaSPAdes (v4.2.0) with default parameters.[104] Quality-controlled reads from each sample were aligned to indexed scaffolds using BWA-MEM (v0.7.17). The resulting SAM files were converted to BAM format and indexed using SAMtools (v1.19.2).[106] MAGs were generated by binning scaffolds using MetaBAT2 (v2.15) (–minContig 2500), using depth files derived from their respective BAM files.[107] MAG quality and taxonomy were assessed using CheckM (v1.2.1) and GTDB-Tk (v2.3.2), respectively.[101,108] Only MAGs identified as *Lactobacillus* by CheckM and *Enterococcus faecalis* by GTDB-Tk were used for downstream analyses. Medium (≥50% completeness, ≤10% contamination) and high (≥90% completeness and ≤5% contamination) quality *E. faecalis* MAGs (Data S5) were used. Average depth of coverage for each MAG was calculated by aligning quality-controlled reads to their binned scaffolds using BWA-MEM and averaging per-base depth calculated with SAMtools depth. *E. faecalis* virulence factors were determined with the BLAST of the virulence factor database (downloaded June 7, 2024) with 99% ID threshold.[57] Whole genome assemblies and MAGs were both used. Samples with fewer than 50,000 post-processed reads were excluded from all metagenomic analyses. Sequencing data from two grossly contaminated sequencing runs was excluded from microbiota analysis, but animal outcomes were included (Data S3).

QUANTIFICATION AND STATISTICAL ANALYSIS

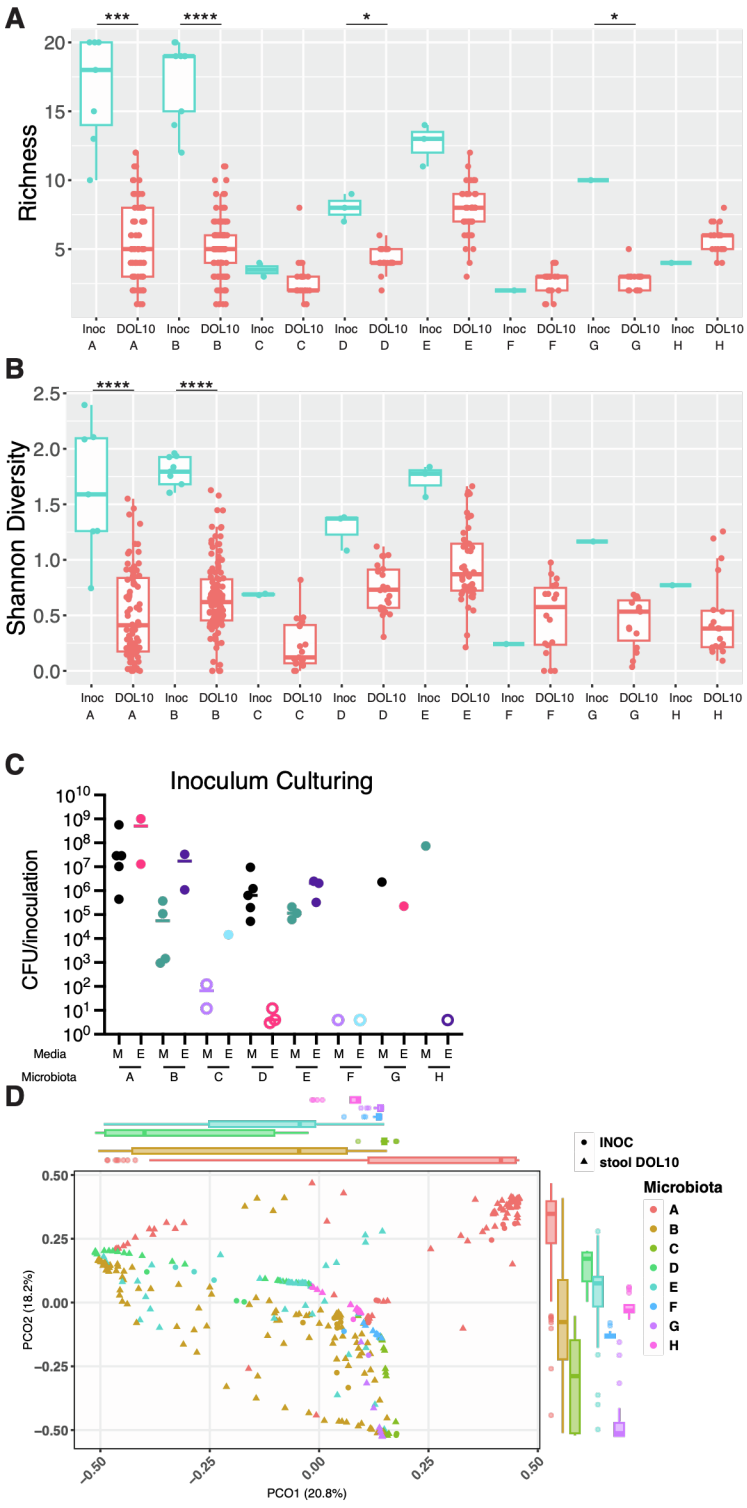
Data processing and analysis were performed in GraphPad Prism v10, R studio V2024.09.1-V2026.05.1 and R v4.4.2–4.6.0. Statistical differences in mouse survival were determined using Log -rank test with pairwise *p* values corrected with the Benjamini-Hochberg (BH) correction for comparisons including >3 groups and $q < 0.1$ considered significant. Statistical differences in microbiota richness and diversity, serum cytokines, gut permeability assays, and bacterial CFUs were determined with Kruskal-Wallis (KW) test with post-hoc Dunn's correction corrected for pairwise comparisons for each analysis. Differences in human plasma cytokines were determined with a Wilcoxon Matched Pairs test with $p < 0.1$ considered significant. RT-PCR data for *panx1* was determined to be normally distributed with a Shapiro-Wilk test and pairwise comparisons were determined with a one-way ANOVA followed by Tukey correction of multiple hypotheses. Differences in microbiota composition were determined with PERMANOVA with the adonis2 package on Bray-Curtis dissimilarity generated from labDSV. PERMANOVAs were performed with 999 permutations. MaAsLin3 was used to determine microbiota associations with survival in mice and meropenem exposure in humans using default settings with Benjamini-Hochberg corrected false discovery $q < 0.1$ as significant per default parameters.[47] For within microbiota comparisons in gnotobiotic mice, the "evaluate_only" flag was set to "abundance". $p < 0.05$ was used as the significance threshold in other analyses. n for analyses represents individual mice and/or fecal samples for metagenomic analysis. Statistical analysis details can be found in figure legends and in Data S4. Symbols for statistical analysis \$, $q < 0.1$; *, $q < 0.05$; **, $q < 0.01$; ***,$q < 0.005$; ****, $q < 0.0001$; and *, $p < 0.05$; **,$p < 0.01$; ***, $p < 0.005$; ****, $p < 0.0001$.

Cell Reports Medicine, Volume *7*

Supplemental information

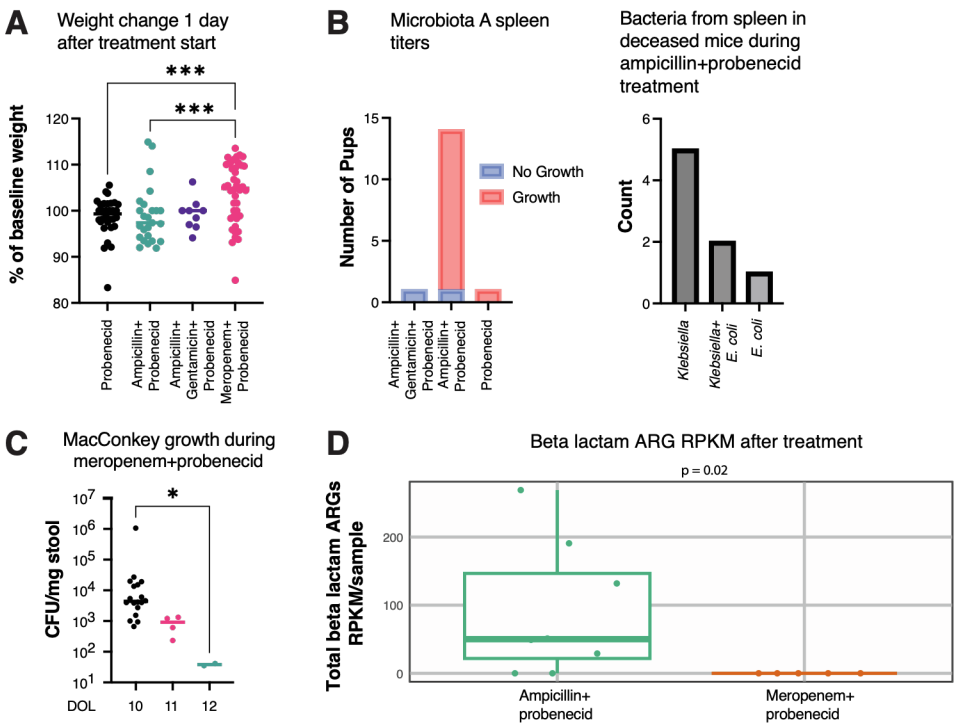
Microbiome-antibiotic-immune interactions influence mortality in preterm infant gut microbiota-humanized gnotobiotic mice

Drew J. Schwartz, Galen G. Wong, Kate E. Wardenburg, Isabel R. Erickson, Jessica Tung, Jie Ning, Lingxia Zhao, Nitan Shalon, Alaric W. D'Souza, Aura Ferreiro, Rachel B. Silverstein, Terence S. Crofts, Carla Hall-Moore, Meghan A. Wallace, John I. Robinson, Jeffrey P. Henderson, Carey-Ann D. Burnham, Barbara B. Warner, Phillip I. Tarr, and Gautam Dantas

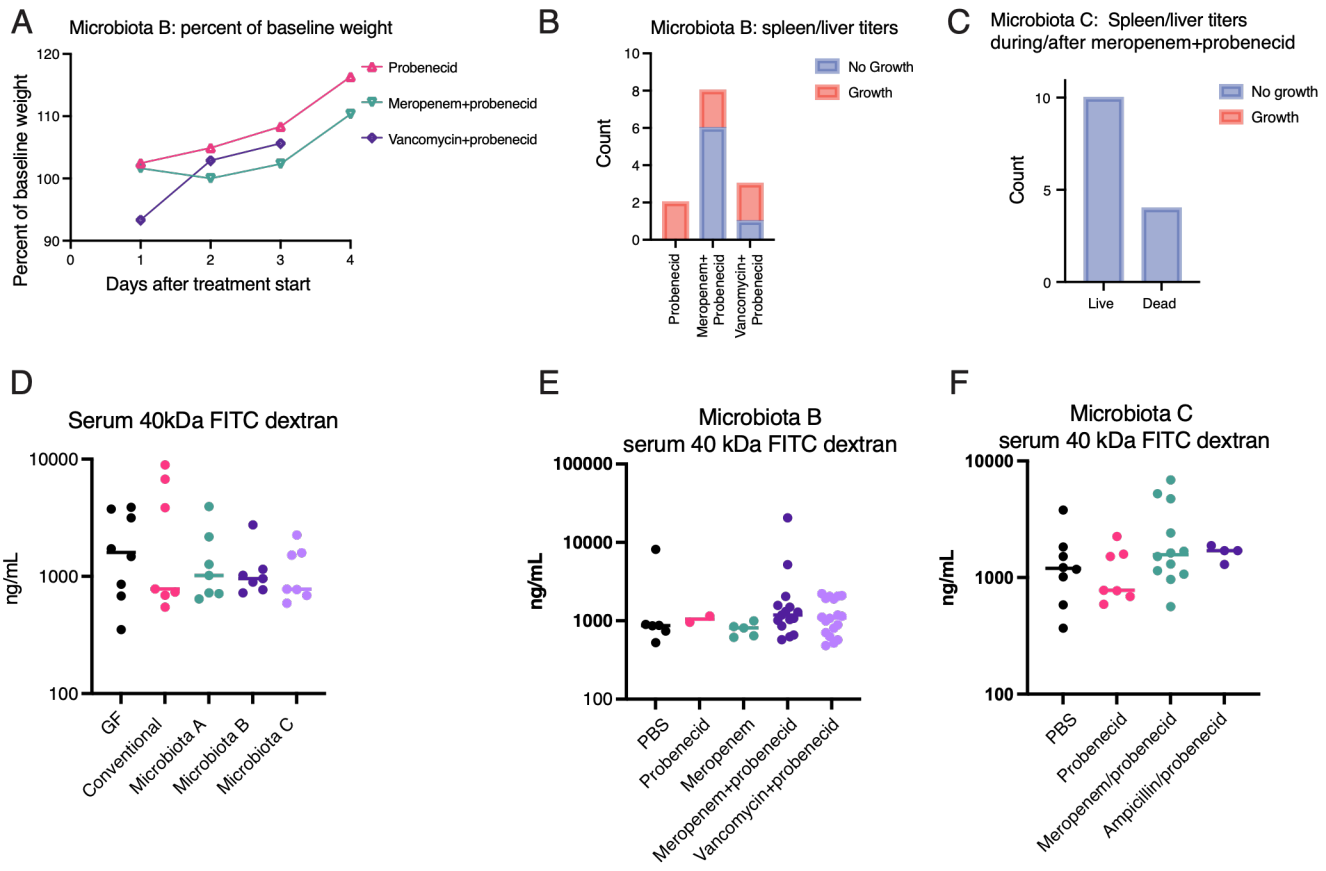


Supplementary Figure 1. Representative microbiota from human infants colonizes germ-free dams, Related to Figure 2. A) Richness and B) Shannon diversity are plotted for inoculum from human infant (blue) and pups (teal) from stool at DOL 10. C) Inocula used to colonize dams was plotted to MacConkey and Enterococcosel agar. Open shapes reflect samples at the limit of detection. D) PCoA of Bray-Curtis dissimilarity of species composition of inocula (circles) and stool (triangles) from pups on DOL 10 depending on

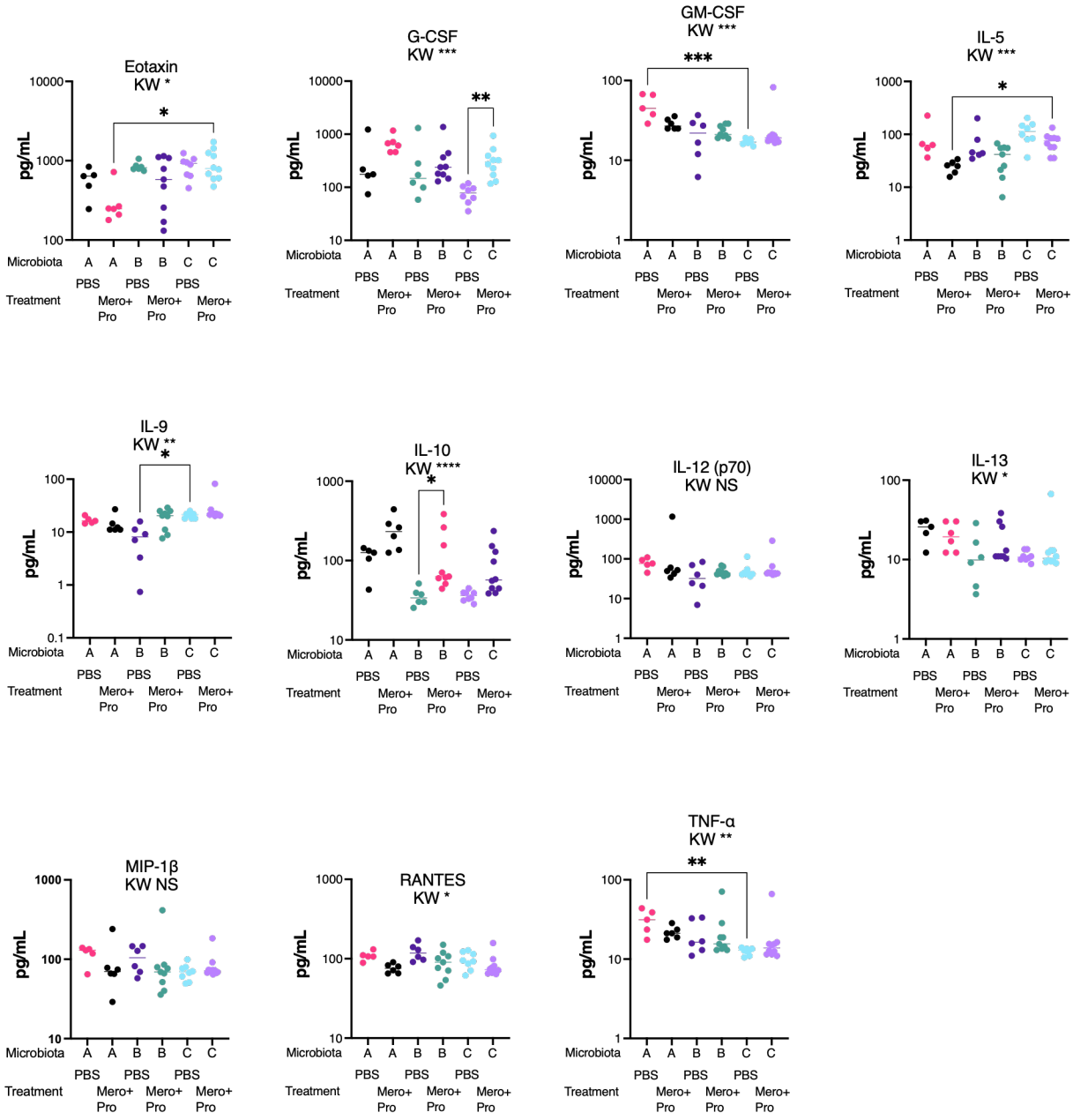
microbiota colonizing dams. Variance explained in parenthesis in the x- and y-label. The distribution of points in principal coordinates 1 and 2 are displayed above and to the right of the graph, respectively. Overall PERMANOVA $p>0.05$. Individual PCO BH-corrected p values in Data S4.



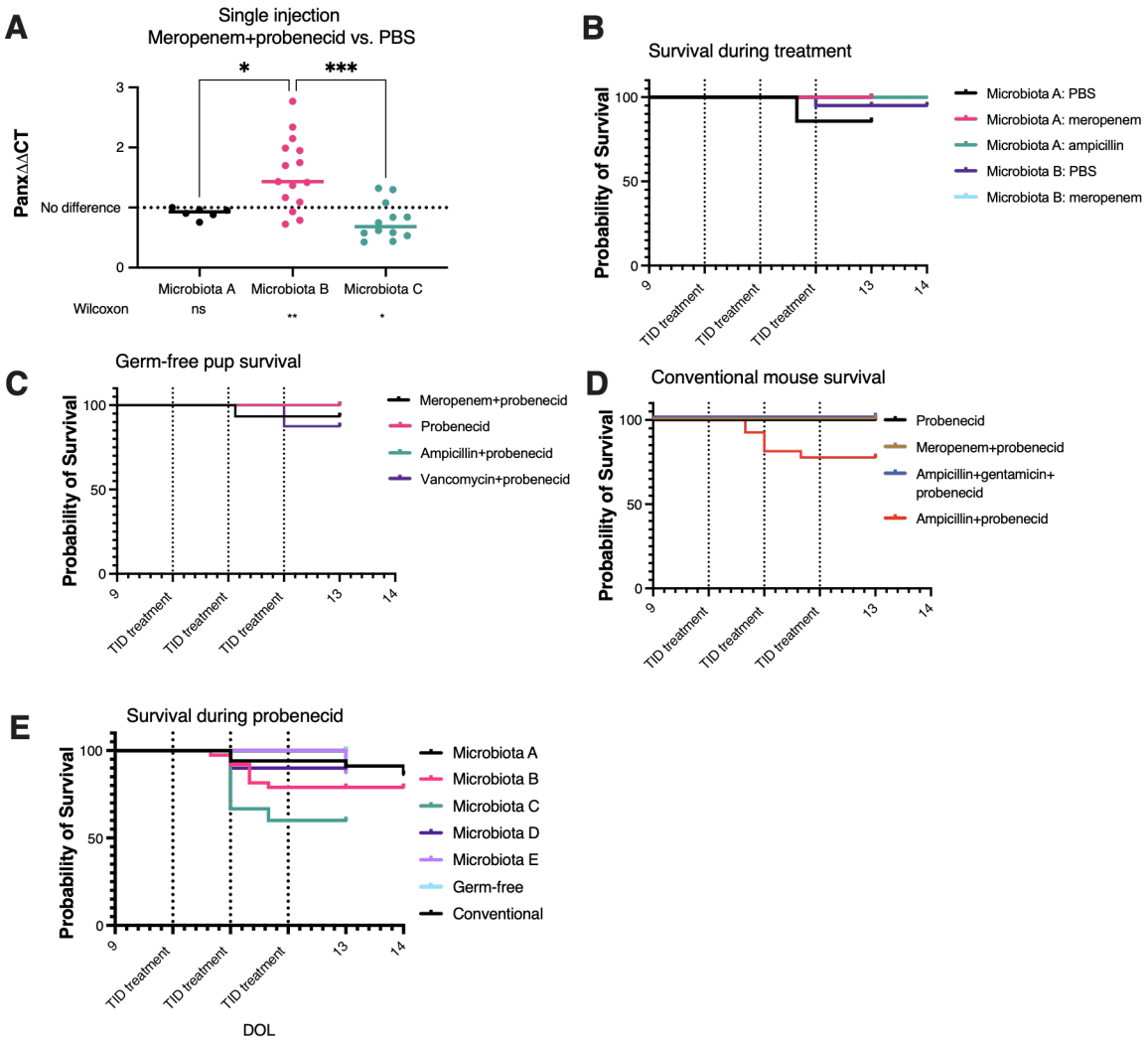
Supplementary Figure 2. Microbiota A-humanized pups have varied responses to antibiotic treatment, Related to Figure 2. A) Percent of baseline weight one day after treatment initiation. KW followed by Dunn's multiple comparison test. B) Growth of bacteria from spleen of deceased animals found intact during treatment and MALDI identification of those colonies. An additional 7 animals treated with ampicillin+probenecid, 4 animals treated with ampicillin+gentamicin+probenecid, and 3 probenecid-treated animals were found cannibalized and therefore excluded. C) Growth of bacteria from fecal samples isolated at the indicated day of life during treatment. KW followed by Dunn's multiple comparison test. Mann-Whitney U test. *, $p<0.05$. D) B-lactam ARGs detected in stool and colon wash metagenomes after 3d of q8h treatment.



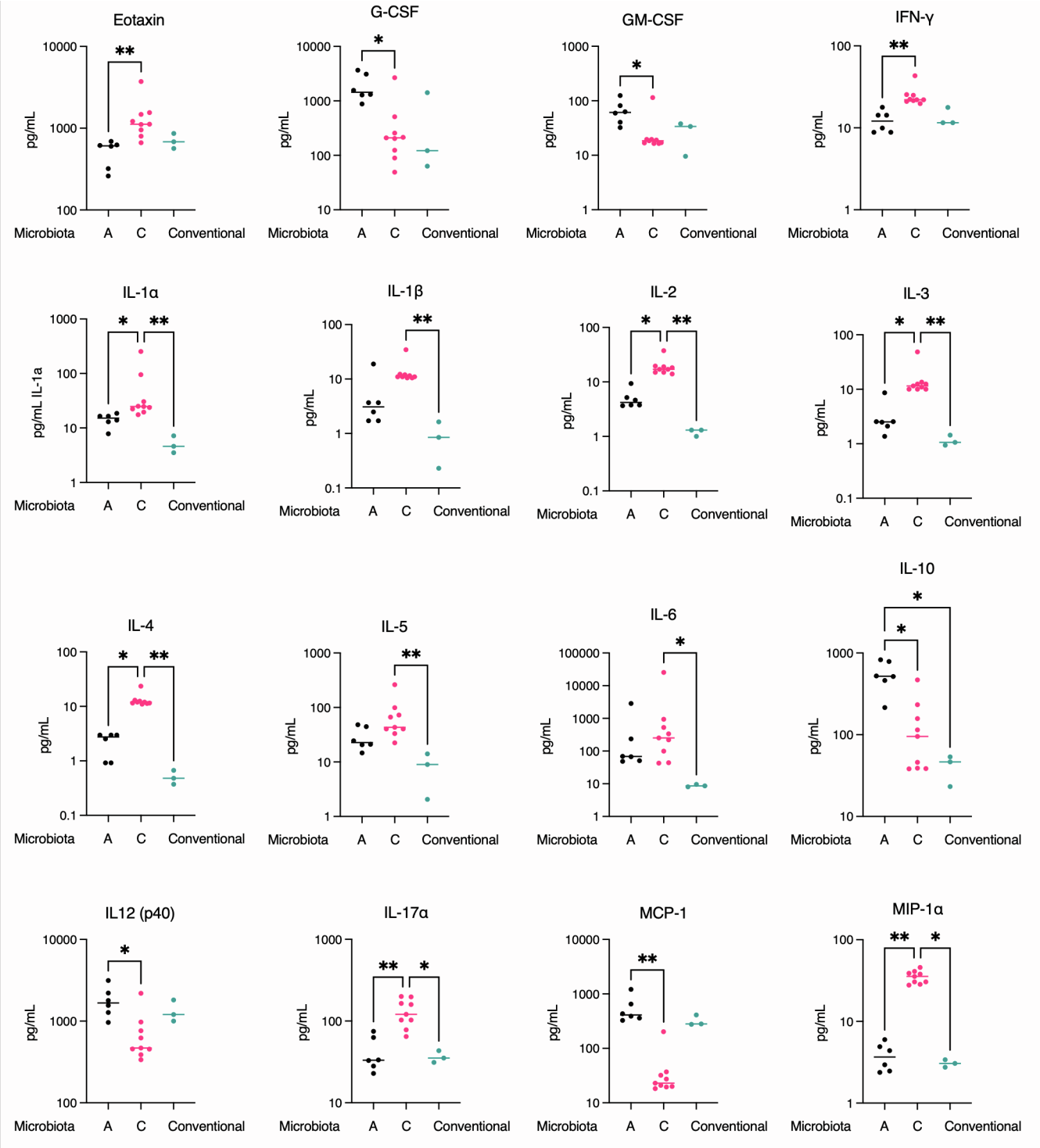
Supplementary Figure 3. Microbiota B- and C-humanized pups demonstrate no increase in gut permeability to various treatments, Related to Figure 3. A) Weight gain relative to baseline during treatment for Microbiota B-humanized pups. Data points for animals that died during treatment are included until the time of death. B-C) Growth of bacteria on MacConkey or Enterococcosel agar from spleen or liver in animals found deceased and intact during antibiotic treatment for (B) Microbiota B- and (C) C-humanized pups. D) 40 kDa FITC-dextran concentrations are plotted 4 hours after oral gavage and 6 hours after subcutaneous probenecid injection to DOL 10 pups humanized with the listed microbiota. E) 40 kDa FITC-dextran concentrations are plotted 4 hours after oral gavage and 6 hours after subcutaneous treatment with the listed agents in (E) Microbiota B- and (F) Microbiota C-humanized pups.



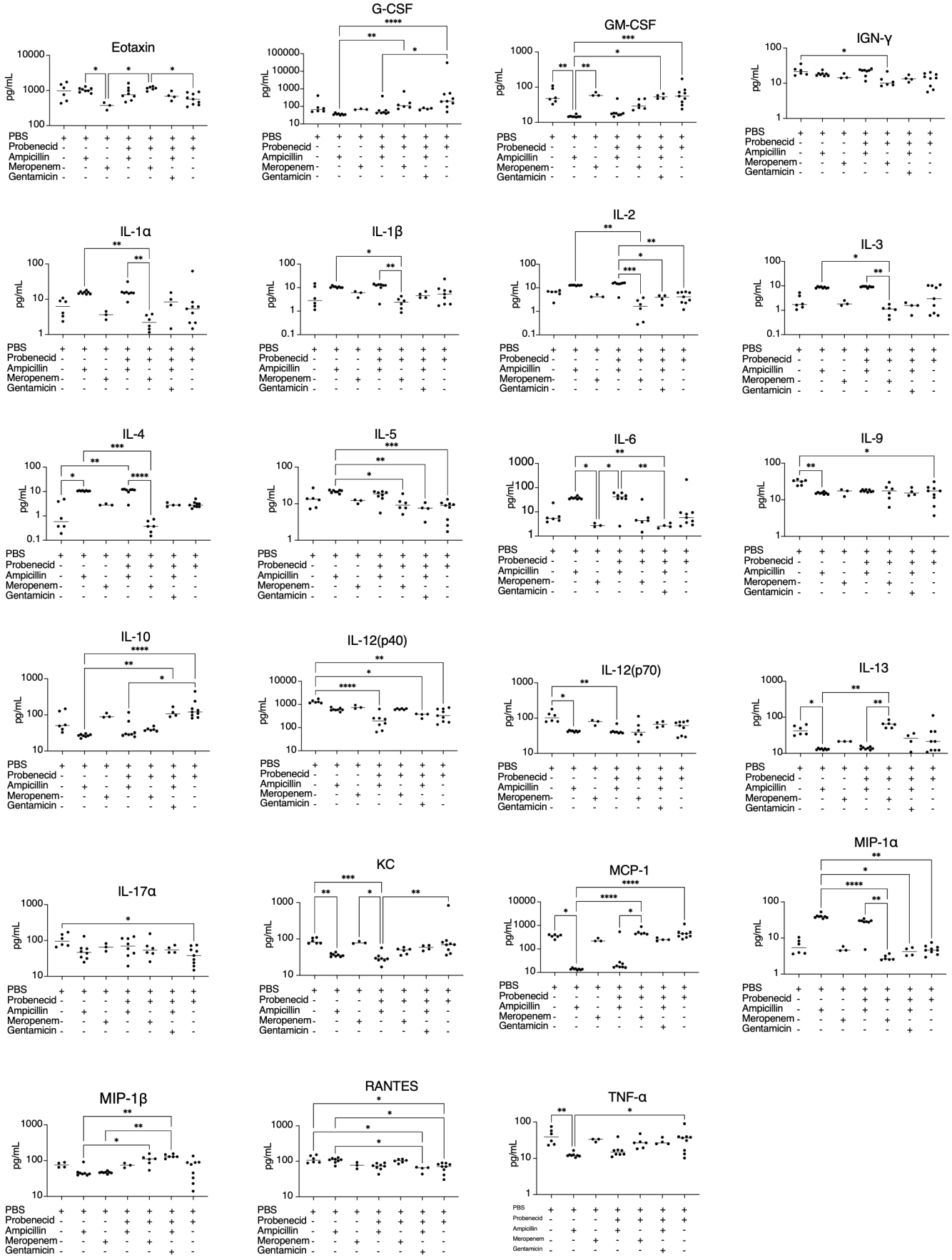
Supplementary Figure 4. Systemic immune dysregulation in Microbiota B- and C-humanized mice treated with meropenem+probenecid, Related to Figure 4. Concentrations of 23 cytokines (remainder in Figure 4) were measured from serum of DOL 10 pups 6 hours after subcutaneous injection with PBS or meropenem+probenecid. Statistical analysis overall with KW test followed by pairwise Dunn's multiple comparison test with hypothesis correction for each cytokine individually. *, $p<0.05$; **, $p<0.01$; ***, $p<0.005$; ****, $p<0.001$, NS = not significant.



Supplementary Figure 5. Probenecid treatment results in different survival and colonic and systemic responses depending on microbiota, Related to Figures 3 and 4. A) ΔΔCT value for *panx1* transcript is plotted from colon RNA from pups with the indicated microbiota 6 hours after single injection of meropenem+probenecid or PBS. *, $p<0.05$; **, $p<0.01$; ***, $p<0.005$, pairwise comparisons with ANOVA with post-hoc Tukey and deviation from null of 1 determined with Wilcoxon Signed Rank. B) Mouse pup survival of Microbiota A- and B-humanized pups during 3 days of q8h treatment with the listed treatments. N=1-3 experiments with 3-20 total mice per group. NS with Logrank test. C) Survival of germ-free mouse pups treated q8h for 3 days of the indicated treatments. N=1-3 experiments 5-15 total mice per group. NS with Logrank test. D) Survival of conventional pups and pups of Germ-free dams colonized with fecal material of conventional mice. N = 1-3 experiments with 5-21 mice per group. NS Logrank test. E) Survival of mouse pups with the listed microbiota during probenecid treatment. N =1-6 experiments with 5-39 mice per group.

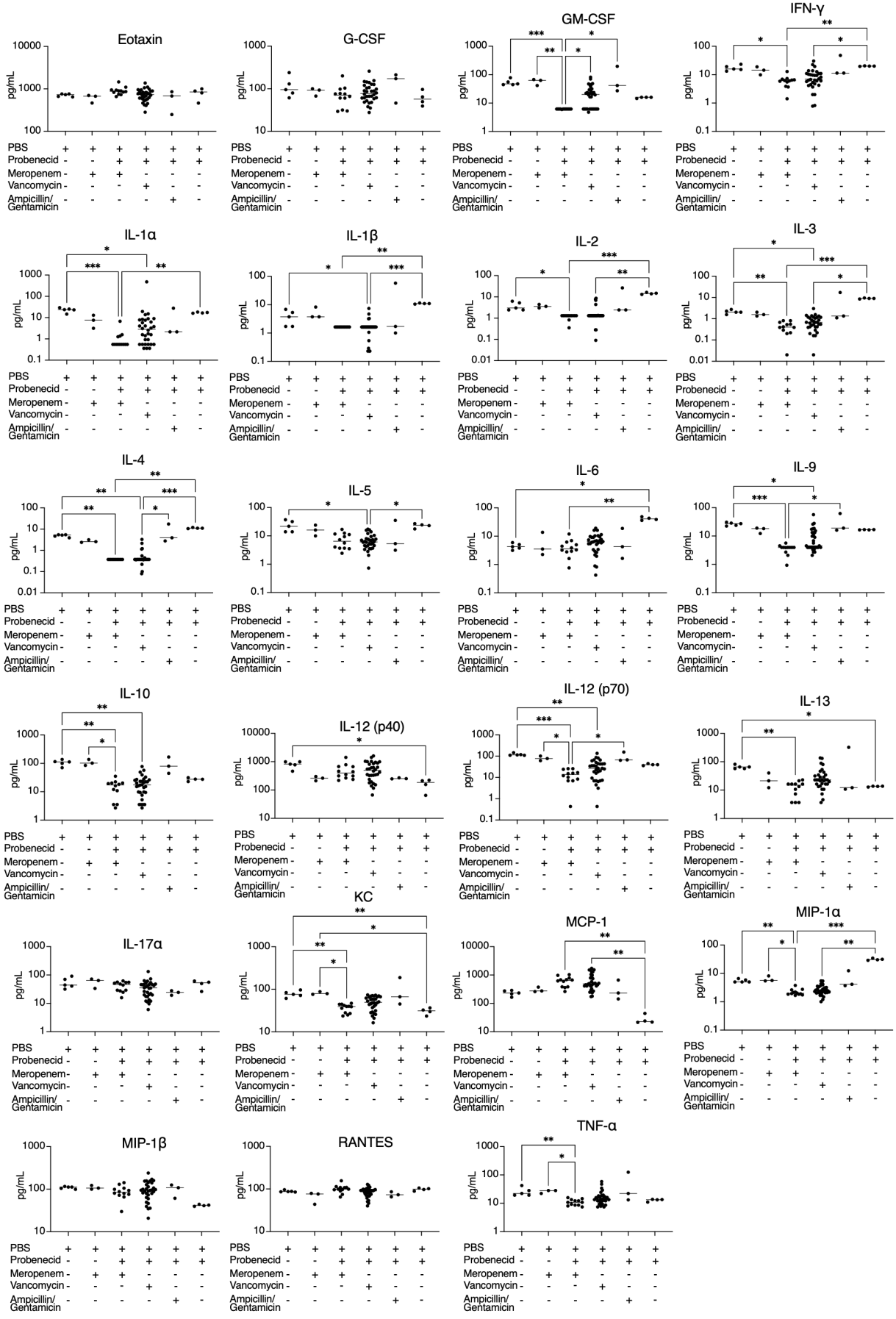


Supplementary Figure 6. Meropenem+probenecid is associated with different cytokine responses depending on the colonizing microbiota, Related to Figures 3 and 4. Concentrations of 23 cytokines were measured from serum of DOL 10 pups 6 hours after subcutaneous injection with meropenem+probenecid. Statistical analysis overall with KW test followed by pairwise Dunn's multiple hypothesis correction. *, $p<0.05$; **, $p<0.01$; ***, $p<0.005$; ****, $p<0.001$. Statistical analysis in Data S4.

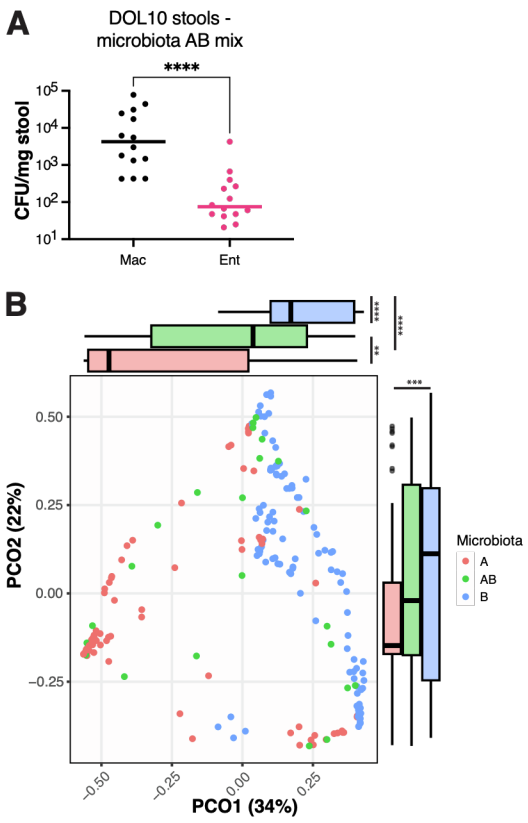


Supplementary Figure 7. Antibiotic+probenecid has increased systemic immune effects beyond antibiotics or probenecid alone in Microbiota A-humanized pups, Related to Figures 3 and 4. Concentrations of 23 cytokines were measured from serum of DOL

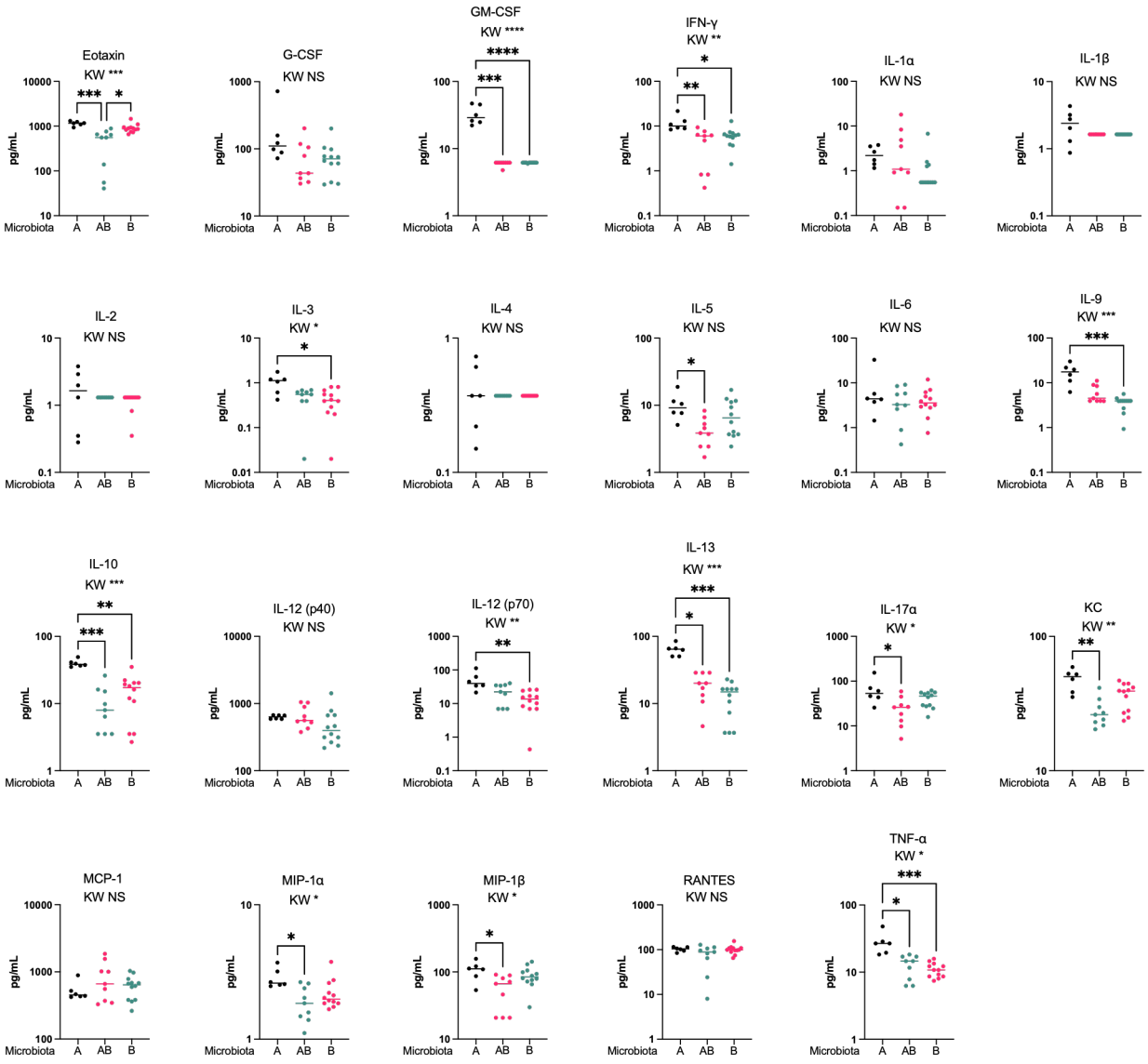
10 pups 6 hours after the listed subcutaneous injections. *, $p<0.05$; **, $p<0.01$; ***, $p<0.005$; ****, $p<0.001$. Statistical analysis in Data S4.


Eotaxin
G-CSF
GM-CSF
IFN-γ
IL-1α
IL-1β
IL-2
IL-3
IL-4
IL-5
IL-6
IL-9
IL-10
IL-12 (p40)
IL-12 (p70)
IL-13
IL-17α
KC
MCP-1
MIP-1α
MIP-1β
RANTES
TNF-α
pg/mL
PBS
Probenecid
Meropenem
Vancomycin
Ampicillin/ Gentamicin

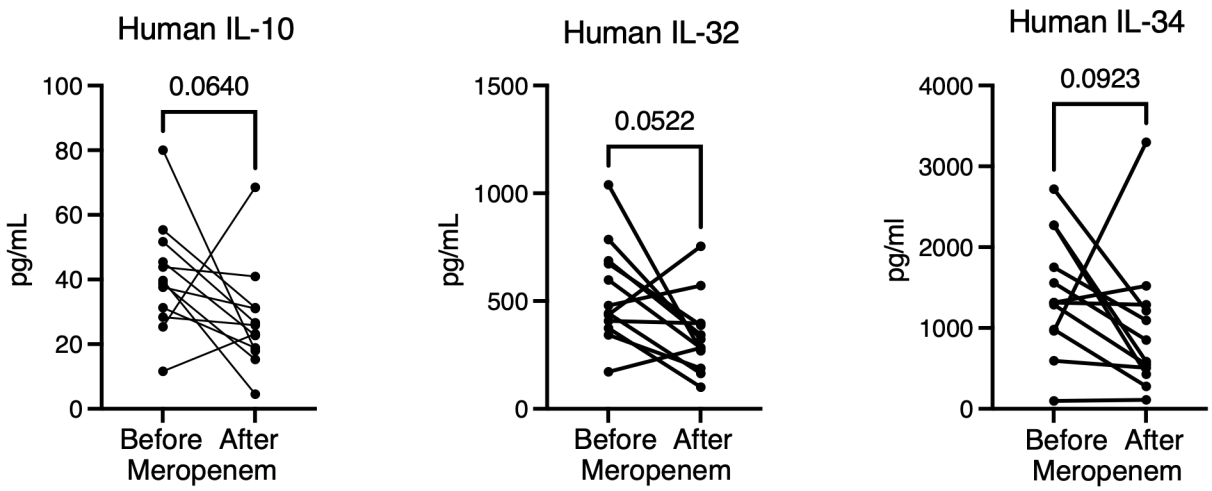
Supplementary Figure 8. Antibiotic+probenecid has increased systemic immune effects beyond antibiotics or probenecid alone in Microbiota B-humanized pups, Related to Figures 3 and 4. Concentrations of 23 cytokines were measured from serum of DOL 10 pups 6 hours after the listed subcutaneous injections. *, $p<0.05$; **, $p<0.01$; ***, $p<0.005$; ****, $p<0.001$. Statistical analysis in Data S4.



Supplementary Figure 9. Microbiota AB-mix humanized pups demonstrate intermediate composition from Microbiota A- or B-humanized pups, Related to Figure 5. **A)** Fecal samples from pups whose dams were humanized with Microbiota AB-mix were plated on MacConkey and Enterococcosel agar. ****, p<0.0001, Mann-Whitney U test. **B)** PCoA of Bray-Curtis dissimilarity is plotted for fecal samples from pups at DOL 10 from Microbiota A-, B-, or AB-mix. Variance explained by each PCO displayed in parenthesis. PERMANOVA >0.05 overall. P values within PCO1 and PCO2 determined with BH-corrected pairwise Wilcoxon test. **, p<0.01; ***, p<0.005; ****, p<0.001.



Supplementary Figure 10. Microbiota AB-mix mice treated with meropenem+probenecid demonstrate serum immune responses alike and different from either Microbiota A- or B-humanized mice, Related to Figure 5. Serum from pups at experimental endpoint on DOL 13 after 3d q8h meropenem+probenecid was profiled with the BioPlex 23-plex cytokine array. Significant differences for each cytokine were determined with KW test followed by Dunn's multiple comparison test. *, $p<0.05$; **, $p<0.01$; ***, $p<0.005$; ****, $p<0.001$.



Supplementary Figure 11. Meropenem decreases concentrations of key cytokines in the plasma of human preterm infants, Related to Figure 6. The concentration of 37 cytokines was determined in plasma before and after meropenem from 12 human preterm infants. Exact p value determined with a paired two-tailed Wilcoxon is listed above the comparison.